A database solution for the quantitative characterisation and comparison of deep-marine siliciclastic depositional systems

Sophie Cullis*[a], Marco Patacci[a], Luca Colombera[a], Laura Bührig[a] and William D. McCaffrey[a]

[a]Turbidites Research Group, University of Leeds, LS2 9JT, Leeds, UK
*Corresponding author: eesle@leeds.ac.uk

Abstract

In sedimentological investigations, the ability to conduct comparative analyses between deep-marine depositional systems is hindered by the wide variety in methods of data collection, scales of observation, resolution, classification approaches and terminology. A relational database, the Deep-Marine Architecture Knowledge Store (DMAKS), has been developed to facilitate such analyses, through the integration of deep-marine sedimentological data collated to a common standard. DMAKS hosts data on siliciclastic deep-marine system boundary conditions, and on architectural and facies properties, including spatial, temporal and hierarchical relationships between units at multiple scales. DMAKS has been devised to include original and literature-derived data from studies of the modern sea-floor, and from ancient successions studied in the sub-surface and in outcrop.
The database can be used as a research tool in both pure and applied science, allowing the quantitative characterisation of deep-marine systems. The ability to synthesise data from several case studies and to filter outputs on multiple parameters that describe the depositional systems and their controlling factors enables evaluation of the degree to which certain controls affect sedimentary architectures, thereby testing the validity of existing models. In applied contexts, DMAKS aids the selection and application of geological analogues to hydrocarbon reservoirs, and permits the development of predictive models of reservoir characteristics that account for geological uncertainty. To demonstrate the breadth of research applications, example outputs are presented on: (i) the characterisation of channel geometries, (ii) the hierarchical organisation of channelised and terminal deposits, (iii) temporal trends in the deposition of terminal lobes, (iv) scaling relationships between adjacent channel and levee architectural elements, (v) quantification of the likely occurrence of elements of different types as a function of the lateral distance away from an element of known type, (vi) proportions and transition statistics of facies in elements and beds, (vii) variability in net-to-gross ratios among element types.

Key words

Deep water; turbidite; channel; lobe; sedimentary architecture; analogue; hydrocarbon reservoir.

1. Introduction

Deep-marine siliciclastic systems remain an attractive topic of study, due in large measure to their importance for the hydrocarbon industry (Posamentier & Kolla, 2003; Prather, 2003; Hadler-Jacobsen et al., 2005; Mayall et al., 2006; Weimer & Slatt, 2007a; Zhang et al., 2017). In particular, a considerable research effort has been made to better understand the architectural and facies properties of such systems, and especially the role that external controls play in influencing their development (e.g., Shanmugam & Moiola, 1988; Reading & Richards 1994; Stow & Mayall 2000; Prather, 2003 and Picot et al., 2016). System analogue and classification approaches to understanding such controls have been influential (e.g., Reading and Richards, 1994), but are necessarily oversimplified as they can only be undertaken with consideration of a limited number of controlling factors. In principle, comparative analyses exploiting the large number of studies on deep-marine systems should enable better characterisation of system architecture (and associated facies distributions) under a range of combinations of controls, together with an improved understanding of the geological processes they record. However, the synthesis of sedimentological data from deep-marine systems is hindered by the fact that studies differ with regard to aims, methods of data collection (e.g., outcrop versus seismic), scales of observation and resolution, classification approaches (in relation to architecture, facies and unit hierarchy), and nomenclature (cf. Mutti & Normark, 1987; Mulder & Alexander, 2001; Weimer & Slatt, 2007a; Cullis et al., 2018).

To facilitate comparative analysis a relational database, the Deep-Marine Architecture Knowledge Store (DMAKS), has been developed. This database allows data collation to be carried out in a systematic and standardised manner and can handle large datasets, allowing meaningful comparisons to be made between the different datasets that it stores. The capacity to integrate different datasets from different deep-marine depositional systems would therefore facilitate subsurface prediction, in part by improving the process of analogue selection via quantitative analysis. The database extends an approach originally proposed by Baas et al. (2005) and is aligned with similar endeavours for fluvial and shallow-marine systems (Colombera et al., 2012, 2016). The fluvial and shallow-marine database methodologies have proven the benefits of this approach in sedimentary geology through quantitative outputs (Colombera et al., 2012, 2015, 2016). The aim of this paper is to demonstrate the value of DMAKS as both a fundamental and applied research tool. This will be achieved by:

1- outlining the structure and content of DMAKS, showing how it enables the synthesis and analysis of diverse sedimentological data;
2- demonstrating potential database applications, through showcasing its capabilities in facilitating characterisation of deep-marine systems.

2. Database purpose, design and standard

The Deep-Marine Architecture Knowledge Store (DMAKS) is a relational database that hosts data on deep-marine siliciclastic depositional systems, recording their architectural properties and facies characteristics with consideration of spatial and hierarchical organisation. These data are derived from peer-reviewed publications and also unpublished sources (theses, original field studies), and are coded in a consistent manner through adoption of a database standard that outlines definitions of database entities and data-entry workflows. DMAKS allows digitisation of both the sedimentary architecture of ancient successions and the geomorphological organisation of modern environments. These data are coded as entries within tables organized in a relational schema implemented in a MySQL database management system. DMAKS accounts for geological entities at different scales of observation (e.g., from lithofacies to stratigraphic intervals), which are commonly investigated through different approaches (e.g., facies and architectural analysis of outcropping successions, bathymetric surveying of modern sea floors). A summary of the geological entities considered in DMAKS and their relationships is presented in Fig. 1.

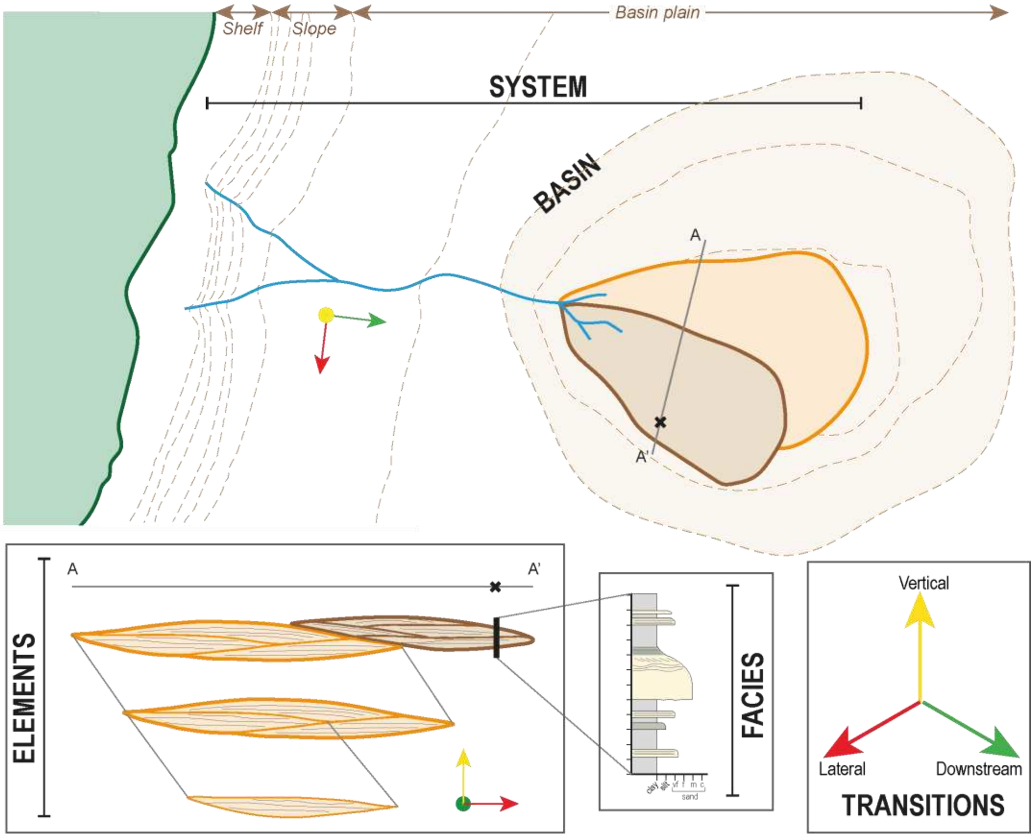

Fig. 1. Conceptual model showing the geological entities stored in DMAKS. Elements are digitised at multiple scales and organised hierarchically. Transitions between units are recorded laterally along strike, down-dip (downstream) and vertically. No scale intended.

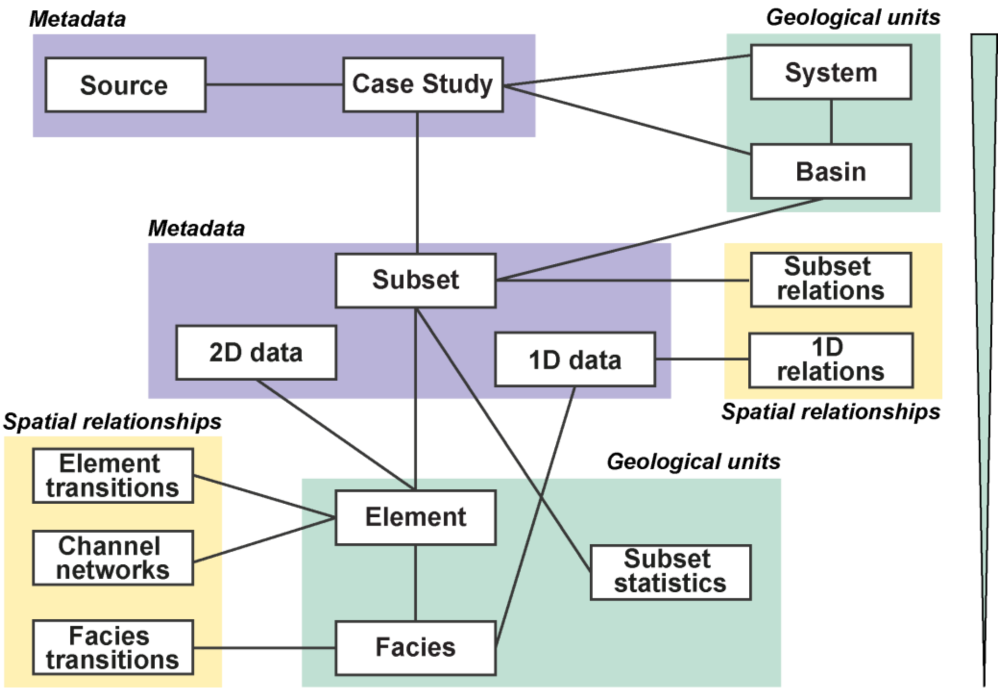

Fig. 2. Representation of the relational schema of DMAKS, showing tables (boxes) and their relationships (connecting lines). For simplicity, look-up tables are not included. The type of data these tables characterise (i.e., geological units, spatial relationships or metadata) are labelled in italics and colour coded. Geological units are arranged in order of descending size.

2.1 Database entities and their relationships

DMAKS currently hosts 18 tables, some of which act as look-up tables for attribute classification. Collectively, these tables store:

i) data on geological units (i.e., sedimentary packages and geomorphological surfaces);
ii) data on spatial relationships between units, in the form of spatial transitions between geological entities of a given type in three dimensions;
iii) associated metadata (e.g., original data types, descriptors of data quality).

Each table contains entries representing multiple instances of a particular type of entity. For example, the ‘Element’ table digitises multiple architectural bodies or geomorphic surfaces, characterised by many attributes. Each entry in a table is given a unique numerical identifier, known as a ‘primary key’, which can be used to link the same entries in other tables as ‘foreign keys’. A graphical summary of the tables and their relationships is presented in Fig. 2.

Data are organised in case studies. A case study can refer to a system, or to a portion thereof, which has been the subject of study by a group of authors, or by more than a group if the studies were intended to be complementary. Alternatively, a case study might include data from multiple deep-marine systems, if such data cannot be unravelled and related to single system entries.

Case studies that include data from one sedimentary system are linked to an entry in the ‘System’ table. In DMAKS, a deep-marine ‘system’ is defined so as to span sedimentary fairways extending from the slope-break to the most distal point of gravity-flow deposition (see Fig. 1). This definition is applied flexibly, in view of the possible need to capture features for which this definition may not apply (e.g., bottom-current deposits); multiple fairways that terminate in the same receiving basin (i.e., topographic depression) are also classified as a single system, e.g., the Santa Monica basin deposits (Normark et al., 2009). In systems that possess a geomorphological expression on the present-day seafloor, active fairways can be readily recognised (e.g., the Zaire fan, Congo-Angola margin; Babonneau et al., 2002). In ancient successions, because of the difficulty in discerning individual fairways, systems generally reflect lithostratigraphic or informal divisions that are commonly accepted in the published literature. DMAKS stores data on the dimensions of a system, its geographic position (and palaeo-position, if applicable), as well as attributes that describe external controls and the geological context (e.g., tectonic setting, source area, shelf width, dominant grain size, feeder type).

A case study can be divided into a number of subset entries. A subset is a set of data that might represent a stratigraphic or planform window or a part of a case study that can be distinguished on the basis of the information it provides. These entries are used to capture the variability in the geological attributes on which a system can be classified and the suitability of the data in a case study. A different subset may be assigned to reflect geographic or stratigraphic subdivisions (e.g., attribution to slope, ramp, or basin-plain settings), variation in attributes that describe external controls, changes in data type, as well as variability in the suitability of the data for certain types of analyses (e.g., for deriving output on unit dimensions, proportions, transition statistics). Ultimately, subsets aid database interrogation. A subset can be linked to data on geological entities directly, or via additional tables (‘2D data’ and ‘1D data’ tables) containing specific metadata when the data are sourced from a 2D or 1D dataset (e.g., cross-sections or logs).

Information on sedimentary basins, smaller sub-basins and individual depocentres is also stored in DMAKS. Attributes include tectonic setting, mechanisms of formation, and geological evolution (e.g., subsidence rates, basin type according to the classification of Ingersoll, 2012) and basin physiography (e.g., basin dimensions, slope gradient, topographic confinement). Through time, different systems might accumulate into the same sedimentary basin (e.g., the Cerro Toro and Tres Pasos Formations into the Magallanes Basin, Romans et al., 2011). However, each ‘basin’ record is created to allow description of the characteristics of the receiving basin during the lifetime of a specific system (see Table 1). In DMAKS, a system may be associated with a number of basins, in cases where the system accumulates over sub-basins consisting of multiple coalescing topographic depressions or depocentres (e.g., the Brazos-Trinity in the Gulf of Mexico, Prather et al., 2012).

Parent-child relationships between basins, sub-basins and depocentres can be recorded in the 'Basin' table.

Currently, DMAKS stores 40 case studies from 29 systems, and 3 multi-system case studies (Table 1, Fig 3).

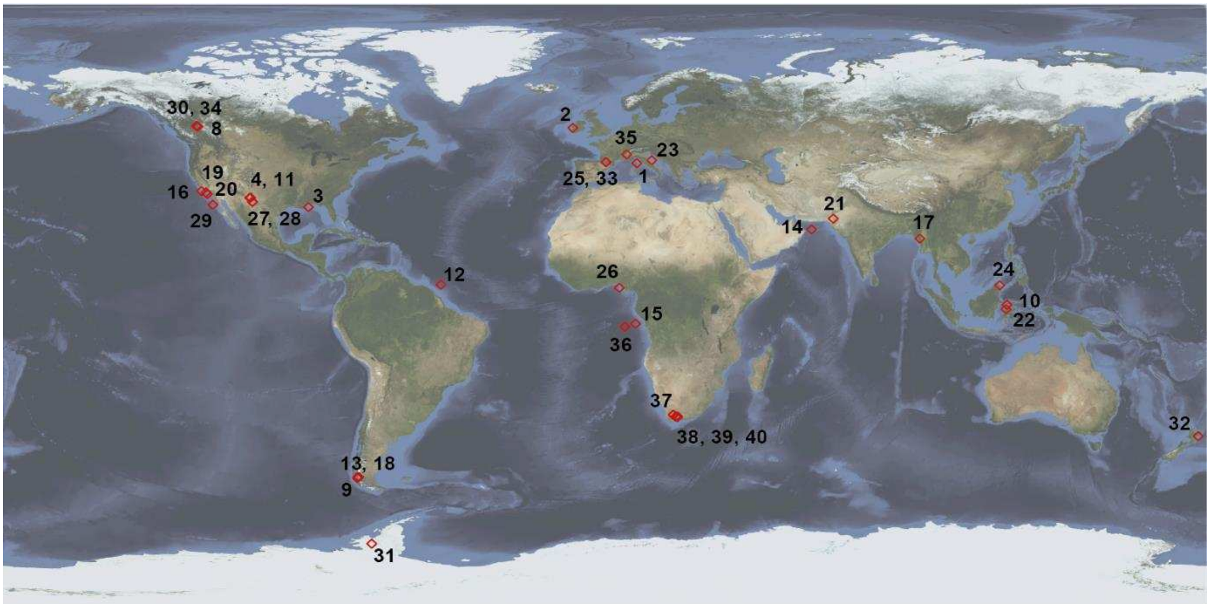

Fig. 3. Map showing the locality of the 40 case studies which relate to a single system, currently included in DMAKS. Numbers correspond to identifiers in Table 1. Image from Stöckli et al. (2005).

	Case study	System	Basin	Literature
1	Late Pleistocene deposits offshore East Corsica, Golo Turbidite System	Golo Turbidite System	Golo Basin	Pichevin et al ., 2003; Gervais et al., 2006(a; b); Deptuck et al., 2008; Prélat et al., 2010; Sømme et al., 2011
2	Ross Sandstone at Loop Head Peninsula and Ballybunnion, Ross Formation	Ross Sandstone Submarine Fan System	Shannon Basin	Pyles 2007; MacDonald et al., 2011
3	Channel-levee system in the DeSoto canyon, NE Gulf of Mexico, Joshua System	Joshua Channel System	-	Posamentier, 2003
4	Channel Complex, Popo Fault Block, Brushy Canyon Formation	Brushy Canyon	Delaware Basin	Beaubouef et al., 1999; Gardner & Borer, 2000; Gardner et al., 2003; Beaubouef et al., 2007*; O'Byrne et* al., 2007(a)
5	Channel dimensions based upon data type taken from McHargue et al., 2011a	-	-	McHargue et al., 2011(a)
6	Channel gradients, continental slope of the Niger Delta taken from McHargue et al., 2011	-	-	McHargue et al., 2011(a); McHargue et al., 2011(b)
7	Channel element thickness based upon gradient taken from McHargue et al., 2011b	-	-	McHargue et al., 2011(b)

8	Isaac Unit 5, Castle Creek area, Isaac Formation	Isaac Formation	-	Arnott, 2007(a; b); Arnott & Ross., 2007; Barton et al., 2007(a); Navarro et al., 2007(a; *b); O'Byrne* et al., 2007(b); Ross & Arnott, 2007; Schwarz & Arnott, 2007; Khan & Arnott, 2011
9	Turbiditic sandstones in the Sierra Contreras, Tres Pasos Formation	Tres Pasos Deep-Water Slope System	Magallanes Basin	Barton et al., 2007(b; c); Armitage et al., 2009; Romans et al., 2011
10	Pleistocene basin-floor offshore E Kalimantan, Kutai Turbidite System	Kutai Pleistocene System	Kutai Basin	Saller et al., 2004; Saller et al., 2008; Sugiaman et al., 2007; Prélat et al., 2010
11	Basin-floor deposits at Willow Mountain, Bell Canyon Formation	Bell Canyon Turbidite System	Delaware Basin	Barton & Dutton, 2007
12	Quaternary Amazon Fan offshore N Brazil, Amazon Turbidite System	Amazon Turbidite System	-	Flood et al., 1991; Piper & Normark, 2001; Jegou et al., 2008
13	Channel-levee deposits Lago Nordenskjold and Laguna Mellizas Sur, Cerro Toro Formation	Cerro Toro Deep-Water System	Magallanes Basin	Bouma, 1982; Barton et al., 2007(b; c)
14	Turbidite lobe architecture from the Oman margin, Al Batha Turbidite System	Al Batha Turbidite System	-	Bourget et al., 2010
15	Modern Deep Sea Fan, offshore Congo-Angola margin, Zaire Turbidite System	Zaire Fan	-	Babonneau et al., 2002; Droz et al., 2003; Marsset et al., 2009; Babonneau et al., 2010
16	Submarine canyons and fans offshore California, Santa Monica Basin	Santa Monica	Santa Monica Basin	Normark et al., 1998; Piper et al., 1999; Piper & Normark, 2001; Normark et al., 2009
17	G-series turbiditic sandstones in the NE Bay of Bengal, Shwe Fan	Bengal Fan	-	Barnes & Normark, 1985; Pickering et al., 1989; Yang & Kim, 2014
18	Condor Channel Belt in the Parque Nacional Torres del Paine, Cerro Toro Formation	Cerro Toro Deep-Water System	Magallanes Basin	Bouma, 1982; Barton et al., 2007(b; c)
19	Black's Beach channel system, La Jolla, California, Scripps & Ardath Formations	Black's Beach	San Diego Basin	May & Warme, 2007; Stright et al., 2014
20	San Clemente slope channel system, California, Capistrano Formation	Capistrano Formation	Capistrano Embayment	Li et al., 2016
21	Channel complexes, Drabber Dhora, Pakistan, Pab Formation	Lower Pab Turbidite System	Pab basin	Eschard et al., 2004; Euzen et al., 2007(a; b); Albuoy et al., 2007
22	Gendalo 1020 Fan, offshore Kalimantan, Miocene System	Gendalo Field	Kutai Basin	Sugiaman et al., 2007; Saller et al., 2008
23	Pleistocene submarine canyon fill, eastern central Italy, Monte Ascensione system	Monte Ascensione system	Peri-Adriatic Basin	Di Celma et al., 2014

24	Outcrop 5 levee-channel turbidites, Papar Highway NW Borneo, West Crocker Formation	West Crocker Fan System	Northwest Sabah Basin	Crevello et al., 2007(a; b; c); Hall, 2013
25	Morillo 1 member channel systems, Ainsa, Morillo Formation	Morillo Turbidite Sub-System	Ainsa Basin	Moody, 2010; Moody et al., 2012; Bayliss & Pickering, 2015
26	Pleistocene canyons, NW Niger Delta, Benin major & Benin minor systems	Continental slope NW Niger Delta	-	Damuth, 1994; Deptuck et al., 2007; Olabode & Adekoya, 2008; Deptuck et al., 2012; Hansen et al., 2017(a)
27	Beacon Channel Complex, Delaware Mountains, Brushy Canyon Formation (data from Beaubouef)	Brushy Canyon	Delaware Basin	Beaubouef et al., 1999; Gardner & Borer, 2000; Gardner et al., 2003; O' Byrne et al., 2007(a); Beaubouef et al., 2007
28	Beacon Channel Complex, Delaware Mountains, Brushy Canyon Formation (data from Pyles)			Beaubouef et al., 1999; Gardner & Borer, 2000; Gardner et al., 2003; O' Byrne et al., 2007(a); Pyles et al., 2010
29	Slope channel system, San Fernado, Mexico, Rosario Formation	San Fernando Turbidite System	San Quintin Sub-basin	Morris & Busby Spera, 1988; Morris & Busby Spera, 1990; Dykstra & Kneller, 2007; Kane et al., 2007; Kane et al., 2009; Kane & Hodgson, 2011; Callow et al., 2013(a; b); McArthur et al., 2016; Hansen et al., 2017(b); Li et al., 2018
30	Isaac channel 3, Castle Creek area, Isaac Formation	Isaac Formation	-	Arnott, 2007(a; b); Arnott & Ross., 2007; Barton et al., 2007(a); Navarro et al., 2007(a; *b); O'Byrne* et al., 2007(b); Ross & Arnott, 2007; Schwarz & Arnott, 2007; Khan & Arnott, 2011
31	Channel-levee complexes, Antarctica, Himalia Ridge Formation	Himalia Ridge Formation Turbidite System	Fossil Bluff Group Basin	Butterworth et al., 1988; MacDonald et al., 1995; Miller & MacDonald, 2004; Butterworth & MacDonald, 2007; Riley et al., 2012
32	Deep-water clastic succession, Taranaki, Urenui Formation	Late Miocene North Taranaki	Taranaki Basin	King & Trasher, 1992; King et al., 1994; King et al., 1996; Arnot et al., 2007(a; b); Browne et al., 2000; Browne et al., 2005; Browne et al., 2007(a; b); King et al., 2007(a; b; c); King et al.,2011; Rotzien et al., 2014; Masalimova et al., 2016
33	Ainsa-1 & Ainsa-2 channel complexes, Huesca, San Vincente Formation	Ainsa Turbidite System	Ainsa Basin	Arbues et al., 2007; Falivene et al., 2010; Pickering & Cantalejo, 2015; Pickering et al., 2015; Scotchman et al., 2015
34	Isaac channel complex 2, S Castle Creek area, Isaac Formation	Isaac Formation	-	Arnott, 2007(a; b); Arnott & Ross., 2007; Barton et al., 2007(a); Navarro et al., 2007(a; b); *O'Byrne* et al., 2007(b); Ross & Arnott, 2007; Schwarz & Arnott, 2007; Khan & Arnott, 2011
35	Champsaur sandstones, Haute Alpes, Grès du Champsaur Formation	Grès du Champsaur Turbidite System	Western Champsaur Basin	Waibel, 1990; McCaffrey et al., 2002; Brunt, 2003; Brunt & McCaffrey, 2007; Brunt et al., 2007; Vinnels et al., 2010

36	Active channel-mouth lobe complex, Congo-Angola margin, Zaire turbidite system	Zaire Fan	-	Droz et al., 2003; Marsset et al., 2009; Dennielou et al., 2017
37	Tanqua Karoo basin floor fan complex (studied by Prélat et al., 2009)	Tanqua Karoo Turbidite System	Tanqua depocentre	Goldhammer et al., 2000; Hodgson et al., 2006; Bouma et al., 2007; Bouma & Delery, 2007; Prélat et al., 2009; Prélat et al., 2010; Kane et al., 2017
38	Unit A proximal basin floor system, Laingsburg Formation	Laingsburg Karoo Turbidite System	Laingsburg depocentre	Sixsmith et al., 2004; Fildani et al., 2007; King et al., 2009; Flint et al., 2011; Prélat & Hodgson, 2013; Hofstra et al., 2015; Spychala et al., 2017; Spychala et al., 2017
39	Unit B & A/B interfan base-of-slope system, Laingsburg Formation			Grecula et al., 2003; Sixsmith et al., 2004; Pringle et al., 2010; Flint et al., 2011; Brunt et al., 2013; Hofstra, 2016
40	Unit C & B/C interfan lower-middle slope system, Fort Brown Formation			Grecula et al., 2003; Sixsmith et al., 2004; Pringle et al., 2010; Di Celma et al., 2011; Flint et al., 2011; Brunt et al., 2013; Morris, 2014; Morris et al., 2016

Table 1. Case studies currently stored in DMAKS and the original source works from which the data have been derived. Basin and system records (if applicable) are also shown. Numbering relates to the order of case study input in DMAKS.

2.1.1 Elements

An 'element' is a geological unit (sedimentary package or geomorphic surface) with a distinct architectural or geomorphological expression, which reflects a particular suite of processes occurring in a specific deep-marine sub-environment. Elements can be nested hierarchically. They are typically discerned in the original sedimentological studies by a combination of descriptive features: geometry, scale, internal facies (characterised in the 'Facies' table, see Section 2.1.2) and relationships with bounding surfaces (e.g., Mutti & Normark, 1987; Pickering et al., 1995; Gardner et al., 2003; Posamentier & Walker, 2006; Terlaky et al., 2016) – characteristics that form the basis of the 'architectural-element analysis' (cf. Miall, 1985).

Architectural units are commonly organised in a hierarchical manner and a variety of hierarchical classification schemes exist in the literature (see review in Cullis et al., 2018). To permit synthesis of different datasets, hierarchical relationships between elements in DMAKS are recorded either by: i) tracking parent-child element relationships, i.e., the containment of a lower-scale element within a higher-scale parent element; ii) tagging the highest-order elements (the largest element unit of a particular 'general' type, see below) and iii) recording the hierarchical assignment made in the source work (see review in Cullis et al., 2018 of the range of approaches that exist); bespoke hierarchical classifications can also be accommodated.

Different element 'types' can be categorised on their interpreted sub-environment of formation, with reliance on interpretations by the authors of the original studies. DMAKS categorises element types in a three-tiered manner based upon the available data and specificity in sub-environment attribution. Element types can be classified according to the following schemes:-

i) element 'depositional style', based upon the unit being either a 'cut (and fill)' or 'accretionary deposit';
ii) 'general element type', an interpretative classification of element sub-environments that largely relies on observational (geometrical and geological) characteristics, applicable over a range of hierarchical scales; all classes are mutually exclusive (Table 2);

iii) ‘detailed element type’, a more specific, interpretational classification of depositional sub-environments; these classes are in some cases restricted to a particular hierarchical level; all classes are mutually exclusive (Table 3).

Element boundaries might be marked by bounding surfaces, or by gradational facies changes (e.g., as an outer-levee deposit interdigitates into background deposition). Channel elements are defined as segments of a channel network bounded by points of channel avulsion or branching (e.g., tributary or distributary channel bifurcation); additionally, channels can be split into multiple channel elements if a change is observed in the depositional style (e.g., a canyon passing downstream to an accretionary channel). Spatial relationships between elements are stored in the ‘Element transition’ or ‘Channel network’ tables (see Section 2.1.4 for detail), the latter only applicable to dip transitions between channel elements. Elements are stored in DMAKS as ‘sedimentary bodies’, ‘geomorphic surfaces’ or ‘mixed’ units (e.g., a parent unit which contains both sedimentary body and geomorphic surface components). Elements are characterised by many attributes, e.g., their 3D geometry, sinuosity, palaeoflow, gradient, age (absolute and relative), style of stacking of internal units, net-to-gross ratio.

General	Description
Channel	An elongate element with negative relief (modern form) or concave-up basal surface (deposit), often observed as the primary pathway of sediment transport in a deep-marine system.
Levee	An aggradational sediment wedge found adjacent to a genetically-related channel. The overbank element forms as sediment-laden flows over-spill their confined sediment pathways.
Scour	Erosional element with negative relief (modern form), or concave-up basal surface (deposit), usually displaying a semi-ellipsoidal (‘scoop’) cross-section, often interpreted as the result of rapid flow expansion or hydraulic jumps.
Lateral splay	An aggradational element formed as sediment-laden channelised flows overtop or breach their banks. This aggradational element can display a lobate or fan-shaped plan-view geometry, expressing a flow direction transverse to the associated confined flow.
Terminal deposit	A depositional body that can display a lens, mounded or sheet 3D geometry. A terminal deposit is found at the terminus of a genetically-related channel architecture.
Mass-transport deposit	An element bound by unconformable surfaces and constituted by remobilised sediments.
Background	A laterally widespread accretionary element composed of very fine grained (clay to silt) sediments from hemipelagic and pelagic fallout.

Table 2. General element type descriptions employed in DMAKS. A scale-independent nomenclature reflecting different sub-environments of deep-marine deposition based upon geometrical and geological (e.g., nature of contacts and facies associations) characteristics. Element types are mutually exclusive; new types can be added to meet available data.

Detailed	Description
Aggradational channel fill	A ‘channel’ element that records vertical accretion (aggradation), with no significant lateral shift in the ‘axial’ part of the deposit.
Lateral-accretion package	Sediment organised in packages that dip towards the axis of a genetically related channel. They are interpreted as the depositional product of the finite lateral migration of a channel.
Master levee	A ‘levee’ element which provides lateral confinement to a channel and is not itself contained within a larger channel.
Overbank terrace	A ‘levee’ element that is contained within a larger-scale channel-form, in some cases bounded by master levees.
Terminal lobe	A lobate or fan shaped plan-view ‘terminal deposit’ geometry. They are composed of multiple facies assemblages that display vertical offset in their stacking, typically in a compensational manner.

Table 3. Detailed element type descriptions used in DMAKS. All elements are mutually exclusive and the list can be expanded to account for new available data and interpretations. This nomenclature builds upon the 'general element types' (Table 2), using process interpretations to inform depositional deep-marine sub-environments.

2.1.2 Facies and beds

The 'Facies' table records the lithological and textural characters of lithofacies or 'facies', the smallest units characterised in the database; each facies unit is contained in a single element. Facies are distinguished where a change is observed in lithology (texture and grain size), grading style, sedimentary or biological structures, palaeoflow direction, or across hiatal surfaces and element boundaries. Each facies record can be tagged as being part of a bed unit, allowing information on 'beds' to also be stored in the Facies table. A bed is defined as a layer of sedimentary rock bounded below and above by either accretionary or erosional bounding surfaces (sensu Campbell, 1967) and deposited by a single flow event, formed by either single- or multi-pulsed flows. The position of a facies within its parent element is recorded via lateral and dip position identifiers, see Section 2.2.2.

Facies attributes include the original facies codes, grain size, sorting, roundness and clast support type (based upon common field notation, cf. Tucker et al., 2011). Grain-size is classified based upon the textural classes of Folk (1980). A textural class is assigned when measured or estimated grain-size distributions allow it. Percentages of grain-size classes based upon granulometric analyses can also be stored when known. The grain size of a sand/sandstone ('S' facies type) can be specified as very coarse to very fine (Wentworth, 1922). The mud, 'M', class of Folk's textural classification (1980) can be further specified into silt/siltstone ('Z') or clay/claystone ('C') categories if possible. When the level of detail for Folk's classes is not provided, facies types can be classified as generic sand/sandstones (_S), mud/mudstones (_M), and gravel/conglomerates (_G).

Sedimentary structures are characterised through a number of attributes. For instance, the general structure of a facies can be classified as 'massive', 'laminated', 'slumped' (when original bedding can be identified) or 'chaotic'. Laminations can be further characterised on their type (planar parallel, non-planar parallel, ripple cross-lamination, cross-stratification, hummocky or wavy), deformation (convoluted, growth structures, flames or unspecified), and clarity (well-developed or faint). In addition, a facies entry can also record information relating to grading, palaeoflow direction, overprinting structures, presence of amalgamation surfaces, trace fossils, clast characteristics (e.g., type, density and orientation), absolute age, etc. The dimensions of facies are also recorded.

Most commonly, facies and their vertical transitions are derived from a measured 1D section (e.g., core, a stratigraphic column or wire-line log). The vertical ordering of facies is thus stored in the Facies table together with information on the facies basal contact (e.g., contact type and geometry).

2.1.3 Aggregate data

In some cases, data are available in the form of statistical summaries that cannot be related to an individual element, bed or facies unit. These data, which describe a group of likewise classified genetic units, are stored in the 'Subset statistics' table. The table records descriptive statistics of unit dimensions, net-to-gross ratios, and transition statistics, linked to a specific subset.

2.1.4 Transitions and relationships

Three-dimensional spatial relationships between adjacent units are stored in DMAKS, as transitions. Transitions between elements are stored in the 'Element transitions' table, except channel-to-channel dip relationships which are stored separately in the 'Channel networks' table. Transitions between facies can be captured in the 'Facies' table in the form of vertical ordering or are stored in the 'Facies transitions' table.

Each transition entry contains the unique identifiers for the two units in question (cf. Colombera et al., 2012, 2016). Transitions can be either vertical (younging), lateral (rightwards when facing downstream) or down-dip (downstream) of the system (Fig. 1). The style of contact across which elements and facies transition can also be documented (e.g., as sharp, sharp erosional, or gradational). Transitions stored in the facies table may also be classed as ‘artificial’ or ‘inferred’, the latter used when a transition is deduced instead of seen. An artificial contact is employed when a facies entry needs to be ‘split’ artificially, for example to map its occurrence at multiple lateral or dip positions in the same element. Classifiers are used to indicate the position where elements are seen to transition, based on the way elements are subdivided along dip and strike (e.g., axis to margin, proximal to distal; see Section 2.2.2). Transitions are stored between all adjacent objects, regardless of hierarchical significance.

The ‘Element transition’ table also accounts for the stacking style of elements, by recording their degree of vertical incision, as well as vertical and lateral offsets. The dip relationships between channel elements, stored in the ‘Channel network’ table, are used to track channel evolution, by recording avulsion nodes, bifurcation points, or confluences.

Spatial relationships between datasets are also digitised in DMAKS. For instance, the ‘Subset relations’ table records transitions between subsets of the same case study, whereas the ‘1D relations’ table records the relative position of 1D datasets.

2.2 Database-wide definitions and common attributes

DMAKS includes both quantitative (e.g., dimensions, sinuosity index) and qualitative data (e.g., basin type, element type). In order to allow comparative analysis, data standardisation is achieved by employing a consistent and repeatable process of data entry. Common attributes across different tables all use the same conventions and units of measure (see Section 2.2.1). Original source-work coding or naming conventions are also stored, allowing the data to be traced back to interpretations in the original source. Text-domain “note” attributes are also included for every table, to allow the inclusion of any additional information.

Metadata are employed throughout the database to record the quality of data stored. For instance, a ‘data quality index’ (DQI) attribute is used to rank the perceived data quality and reliability of interpretations (e.g., element-type classifications), using a three-tiered classification (from A, highest, to C, lowest quality; cf. Baas et al., 2005; Colombera et al., 2012; 2016). DQIs are used to rank the confidence with which attributes can be assigned, based on expert judgement.

2.2.1 Dimensions

Length, width and thickness are all taken with respect to a reference system orientated relative to the dominant local (palaeo-) flow direction, except for levee elements, whose dimensions are measured relative to (palaeo-) flow direction in their genetically related channel. Metadata characterising these measurements are also stored. For example, unit dimensions are classified on the type of measurement, as values may not represent the true maximum element width, length or thickness (see Fig. 4). Dimensions may be incomplete as a product of erosion or because of the spatial limits of the dataset (e.g., outcrop termination). The completeness of element dimensions can be classified as either true, apparent, partial or unlimited, sensu Geehan & Underwood (1993). A ‘spatial type’ attribute classifies the spatial constraints of the dataset from which the measurements have been taken (e.g., whether a ‘true’ value has been recorded from observations in 1D, 2D or 3D).

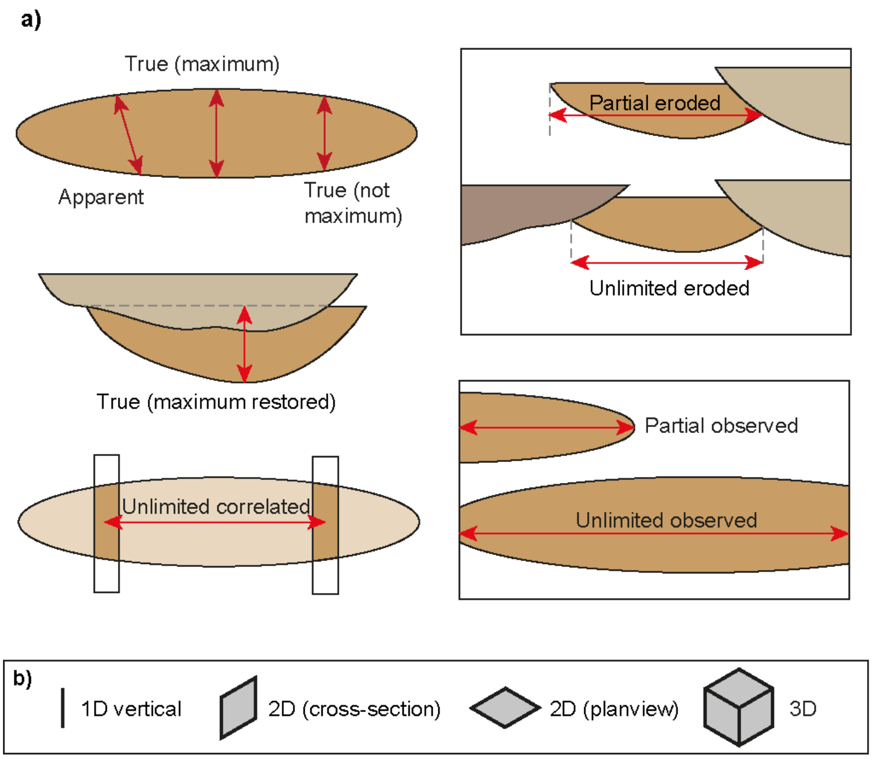

Fig. 4. Dimensional parameters used to characterise element dimensions with respect to a) type of measurements and b) spatial coverage offered by a dataset. The 'true restored' measurement type is only applicable to thicknesses, while the 'unlimited correlated' class is only applicable to width and length values.

2.2.2 Position classifiers

Position classifiers are used to record i) the position across which an element–to-element transition occurs, and ii) the position of a facies within its parent element, to account for lateral variations in facies architecture within elements. Intra-element divisions along strike and dip have therefore been established based upon geometrical rules (Fig. 5). An element is divided into 5 equal portions along its strike width, denoting margin/fringe, off-axis and axis (core) regions. Levee elements are divided into 3 portions based upon the position of their crest peak. The dip length of an element is divided into 3 equal portions, denoting proximal, medial and distal regions. Descriptions of the internal partition of elements based on criteria of facies organisation and as adopted in the source work can be additionally recorded in the 'Facies' table.

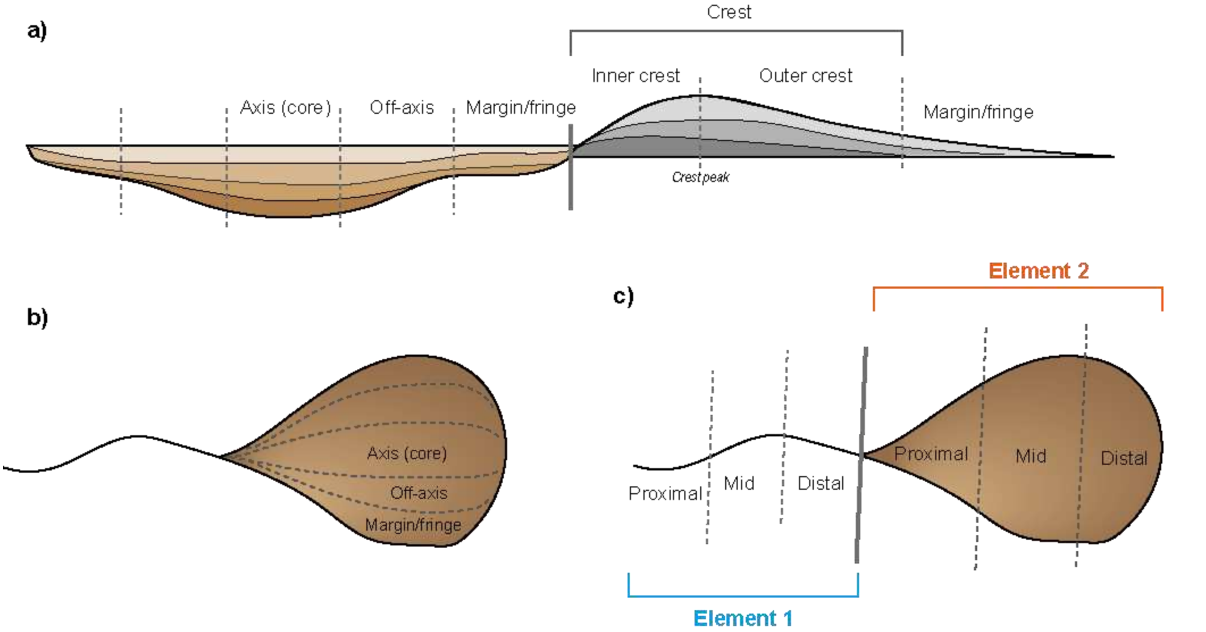

Fig. 5. Position classifiers applicable in the 'Facies', 'Facies transition' and 'Element transition' tables. Lateral intra-element divisions for a) channel, levee and b) terminal deposit architectures are shown. A general 'crest' classifier is used when the levee crest peak is unknown or unclear. The outer crest to margin/fringe boundary is defined as the half-distance between the crest peak and the elements outer termination point. Dip positions in a channel and terminal deposit are shown in part c).

3. Database applications

DMAKS is interrogated through Structured Query Language (SQL). Seven example applications are presented here, based upon quantitative outputs derived from the current database content (Table 1). These examples demonstrate some of the types of analyses that are feasible, and how these can be applied to further our understanding of deep-marine systems. Data upload is ongoing.

3.1 Quantification of element geometries

The ability to integrate data from seismic and outcrop enables dimensional data to be considered across multiple orders of magnitude, bridging the gap between studies conducted at different scales of observation and resolution. For example, Figs. 6 A and B show discrepancies between channel widths described in outcrop vs. seismic or bathymetric studies, which have mean widths of 746 and 1,120 m, respectively.

DMAKS output can be employed to assess trends between geometrical properties, leveraging a wide data pool. For instance, a 10:1 width-to-thickness aspect ratio (resulting in a constant linear relationship of $y = 10x$, where y is width and x is depth) is often cited to be typical for submarine channel-forms and channel bodies, based upon the study conducted by Clark & Pickering (1996; Fig. 6 C). This result is based upon 50 measurements of channel and scour elements associated with a range of hierarchical scales. Weimer & Slatt (2007b) extended upon this proposed trend by suggesting that the channel aspect ratio changes in response to system gradient, resulting in a width-to-thickness ratio of 50:1 down-dip compared to the 10:1 relationship up-dip. Data collected by Konsoer et al. (2013) from 23 modern submarine channels suggests that width-to-depth approximates the 50:1 ratio, whereby channel width (y) varies with depth (x) following a relationship of $y = 47.4x^{0.94}$. However, these channel measurements are a mix taken from both slope and basin-plain environments (Fig. 6 C). DMAKS currently enables comparison of data from 196 channels of all hierarchical scales derived from multiple studies (Fig. 6 C). Based on DMAKS, a positive relationship between channel width and thickness (or depth, in the case of modern forms) is also identified (r^2 =

0.50, Pearson's coefficient = 0.91, p-value <0.001), but with a smaller exponent ($y = 73.7x^{0.61}$) in comparison to the previously proposed trends.

Outputs can be filtered on any boundary conditions, to test relationships between element geometries and possible predictors or controlling factors. For instance, channel elements from sand-rich systems are associated with thinner and narrower channel geometries (Fig. 6 C), supporting the role of controlling factors on which depositional models have been categorised by Reading & Richards (1994) and Normark & Piper (1991). Additionally, channel elements from sand-prone systems show a larger aspect ratio, on average, compared to channels from systems dominated by fine-grained deposits, challenging the findings of Delery & Bouma (2003).

Scatter is observed, over an order of magnitude, about the line of best fit (Fig. 6 C). The geometric variability of channels has been related to the variability that can be found in turbidite flow properties (Wynn et al., 2007; Konsoer et al., 2013; Jobe et al., 2016 and Qin et al., 2016). For example, high-aspect-ratio channel outliers identified in Fig. 6 C are typically associated with weakly confined environments (c.f. spill phases sensu Gardner et al., 2003, or distributary channels sensu Posamentier & Kolla, 2003). This association supports work by Brunt et al. (2013), suggesting that deep-marine channel geometry can be affected by the degree of flow confinement.

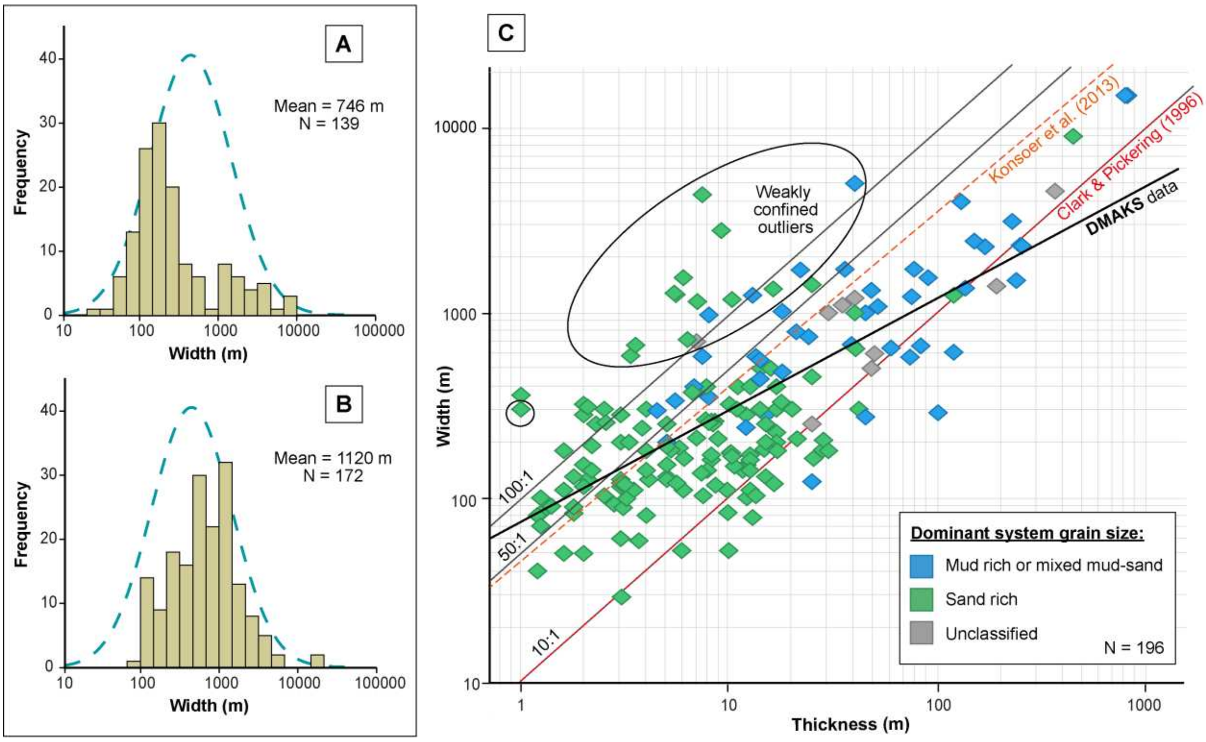

Fig. 6. A-B) Histograms of the measured width of channel elements based upon outcrop (A) and seismic and bathymetric data (B). A lognormal distribution curve fitted to a merge of both datasets is plotted in both graphs (dashed line; population mean = 953 m). Note the logarithmic scale and thus the positive skewness of the data. C) Width vs thickness (or depth, in the case of modern forms) of channel elements. The 10:1 width-to-thickness aspect ratio proposed by Clark & Pickering (1996; red) is plotted, as well as power-law regression lines for the DMAKS dataset (black), and the study by Konsoer et al. (2013; orange). Channels are classified by the dominant grain size for the system, as sand dominated (green), mud dominated or mixed (blue) or unclassified (grey). Outliers above roughly 100:1 are mostly channels documented as showing weak confinement in the original source-work. N = number of channel elements included in each plot. All measurements are true (maximum) values.

3.2 Comparisons of hierarchical organisation

The geological significance of deep-marine hierarchical relationships is not yet fully understood, and its comprehension is in part hindered by the inconsistent use of terminology (Cullis et al., 2018). The interpretational difficulties become evident when element dimensions are plotted against the terminology adopted in the original sources, as in Fig. 7, which demonstrates the size range observed in channel and lobate features sharing the same nominal architectural classification. A large spread in the element dimensions can be seen for each term, even when hierarchical parent-child relationships are considered, as terminology can be associated with multiple ‘parent’ hierarchical orders. Hierarchical terminology reported in source works can therefore be seen to provide no consistent dimensional constraint to element dimensions.

Often, comparisons between units occurring in different deep-marine systems and associated with hierarchical categories involve re-assignment of reported hierarchical classifications to an alternative scheme (e.g., Sprague et al., 2005; Prélat et al. 2010; Straub & Pyles 2012). These comparisons are arguably largely subjective and inherently uncertain. DMAKS permits assessment of how the original terminology relates to nested parent-to-child relationships between elements, and how these hierarchical relationships are reflected in the relative size of the elements (e.g., Fig. 7). Scaling relationships between child and parent elements of both channels and terminal deposits range between 1:1 and 10:1 (Fig. 8). Such information can improve our understanding of the hierarchical organisation of deep-marine systems and has the potential to help inform reservoir models.

DMAKS enables comparisons between architectural elements to be undertaken in a consistent manner, by querying on any combination of empirical attributes, related for example to scale, stratal trends, bounding-surface relationships (Figs. 7 and 8), or facies and architectural characteristics associated with a particular sub-environment. Therefore, DMAKS can be used to make objective comparisons between case studies that use different terminologies or hierarchical definitions. This arguably results in more meaningful analyses of the organisation of sedimentary architecture in deep-marine clastics than what can typically be attempted on the basis of terminologies or the re-assignment of data to classification schemes.

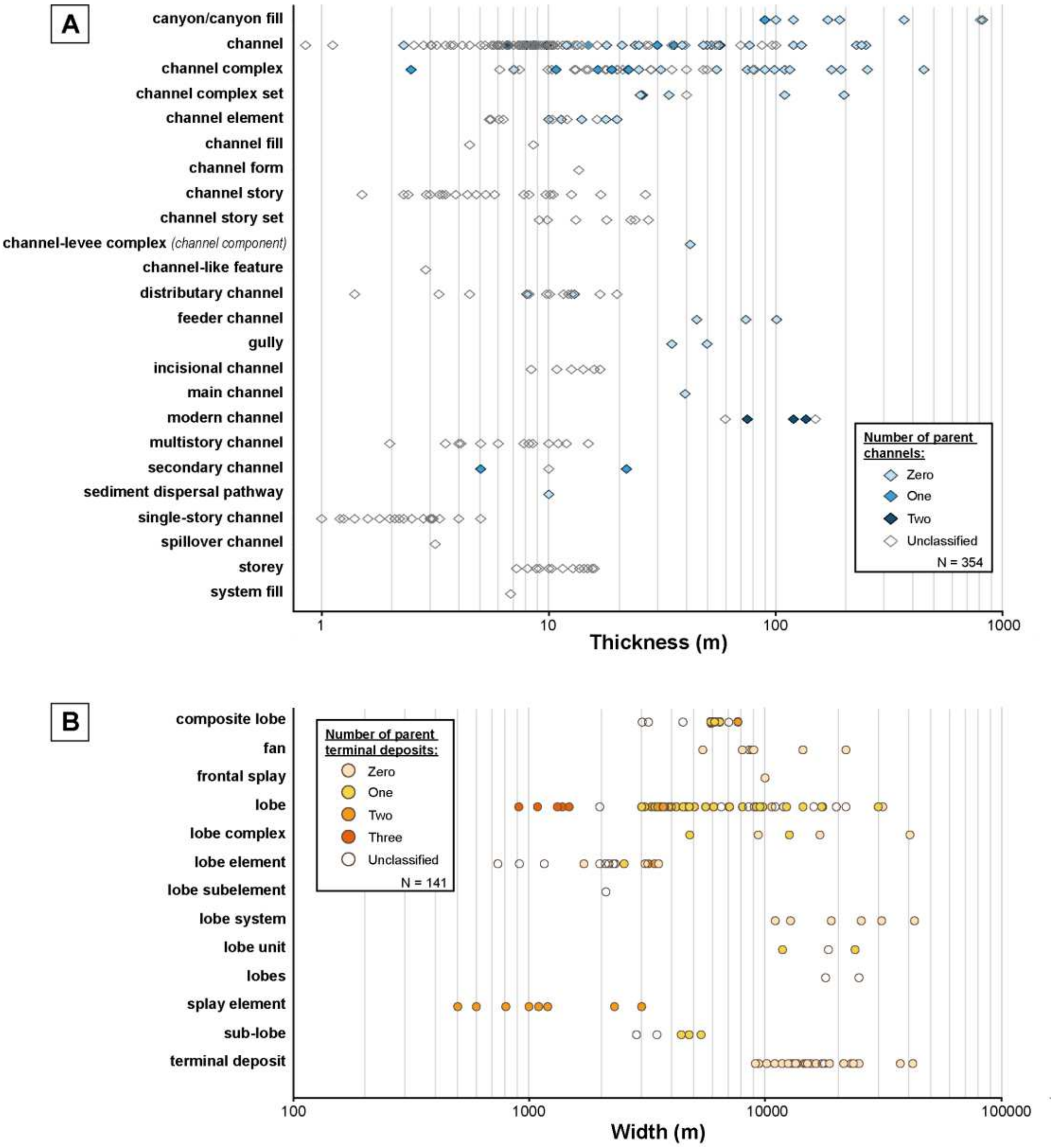

Fig. 7. Channel-element thickness (A) and terminal-deposit width (B) 'true (maximum)' measurements classified by the original source-work terminology. The number of parent elements encapsulating an element is indicated, starting from a known highest-order element (zero).

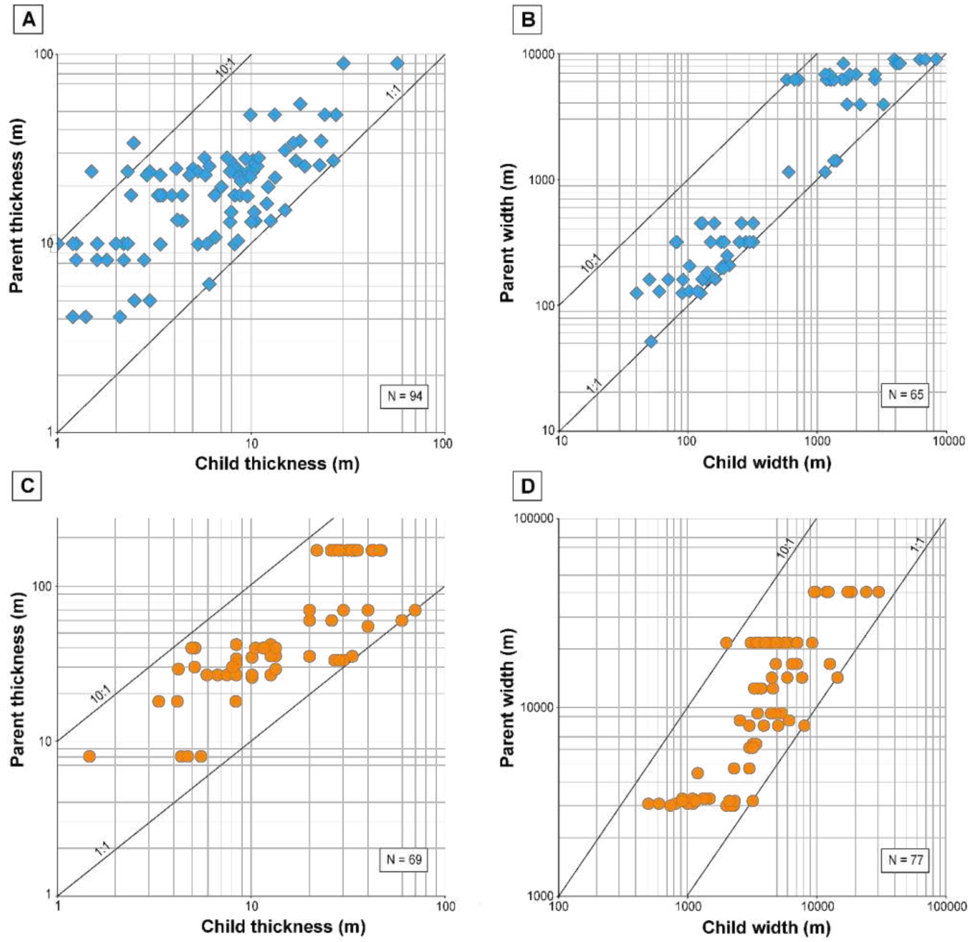

Fig. 8. Relationships between the geometry of 'child' elements and the geometry of the 'parent' elements in which they are contained, for channel elements (blue diamonds, A-B) and terminal deposits (orange circles, C-D). Data are plotted for element thickness (A, C) and width (B, D). Only true (maximum) measurements are considered.

3.3 Characterisation of architectural spatial arrangements

DMAKS allows spatial relationships between architectural units to be recorded in 3D, along the vertical, strike and dip directions. These data can be used to produce information on scaling relationships between co-genetic deposits. For example, Fig. 9 describes the scaling relationship between the width of channel elements and the width of genetically-related laterally adjacent levees. A positive relationship between master levees (i.e., a levee not contained in a larger channel body, see Table 3) and their adjacent channels is depicted ($r^2 = 0.62$), in agreement with the findings of Skene et al. (2002) and Nakajima & Kneller (2013). Filtering the data by physiographic setting suggests that basin-plain environments are associated with wider master levees and channels compared to their slope counterparts, supporting the notion that steeper slopes result in narrower master levees (Nakajima & Kneller 2013). These outputs can be utilised as predictive tools, for example for prediction of thin-bedded volumes and in reservoir modelling.

Additionally, DMAKS can produce outputs that describe the likelihood of occurrence of a certain architectural element away from a known point, as in Fig. 10. Such outputs serve as predictive models that can be used to support conceptual models of the subsurface and guide reservoir-development planning, especially in data-poor situations.

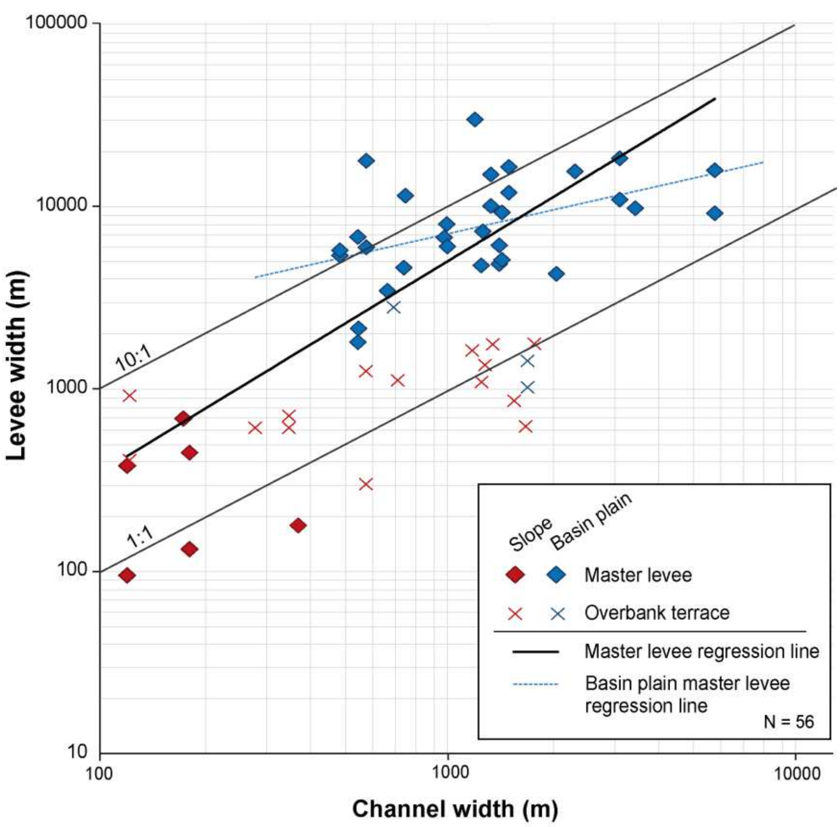

Fig. 9. Cross-plot of the width of channel elements and genetically-related laterally adjacent levees. Levees are further categorised as master levees or overbank terraces (see detailed element type descriptions, Table 3). Elements are classified by depositional setting (red: slope; blue: basin plain). All widths are 'true (maximum)' values. A power-law regression line associated with master levee-channel relationships is shown (bold black line; $y = 1.6x^{1.16}$), as well as a power law regression line for master levee-channel relationships located on the basin plain (blue dashed line; $y=356.2x^{0.43}$, r^2 = 0.22).

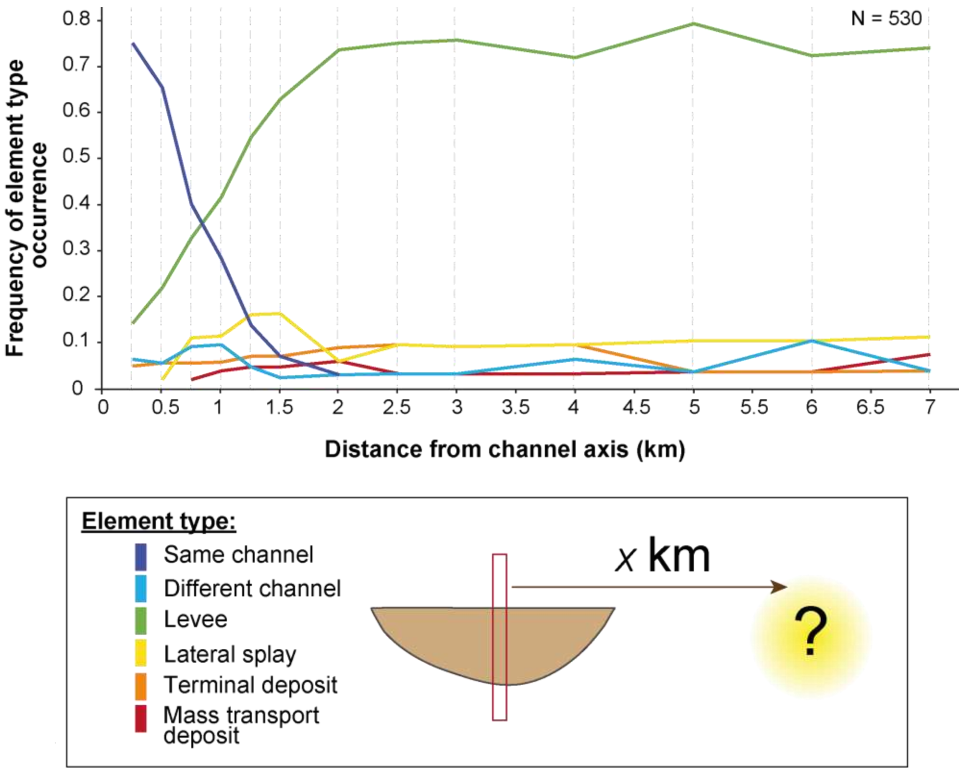

Fig. 10. Plot showing the frequency of different element-type occurrences as a function of the lateral (strike) distance away from the axis of a channel. The channel elements at the origin do not include modern channel forms and are not described in the source-work as a 'complex' or 'storey'. Lateral along-strike transitions (in both directions away from the channel axis) are counted between highest-order elements. N records the total number of element transitions. Grey dashed lines mark the distances at which frequencies were calculated.

3.4 Temporal variations in architecture

Geochronological dating of deep-marine deposits is usually limited with respect to sampling density and resolution, limiting the ability to constrain absolute ages of individual elements. However, the relative depositional age of deposits can often be inferred based upon geological principles of succession. Data on the relative timing of deposition are stored for elements in DMAKS, allowing derivation of outputs that describe how architectural attributes vary in a relative time frame. For example, Fig. 11 shows the change in lobate terminal deposit geometry in terms of length-to-width ratio over time for a number of different subsets. An oscillation through time between more elongate and more equant deposits can be seen in some of the examples, e.g., the South Golo lobe and Kutai basin-plain fan, Fig. 11 A-B. Additional data might provide the basis for testing whether this apparent cyclicity is common in the architecture of turbidite lobes and sheets, and might elucidate whether this could reflect a form of autogenic organisation.

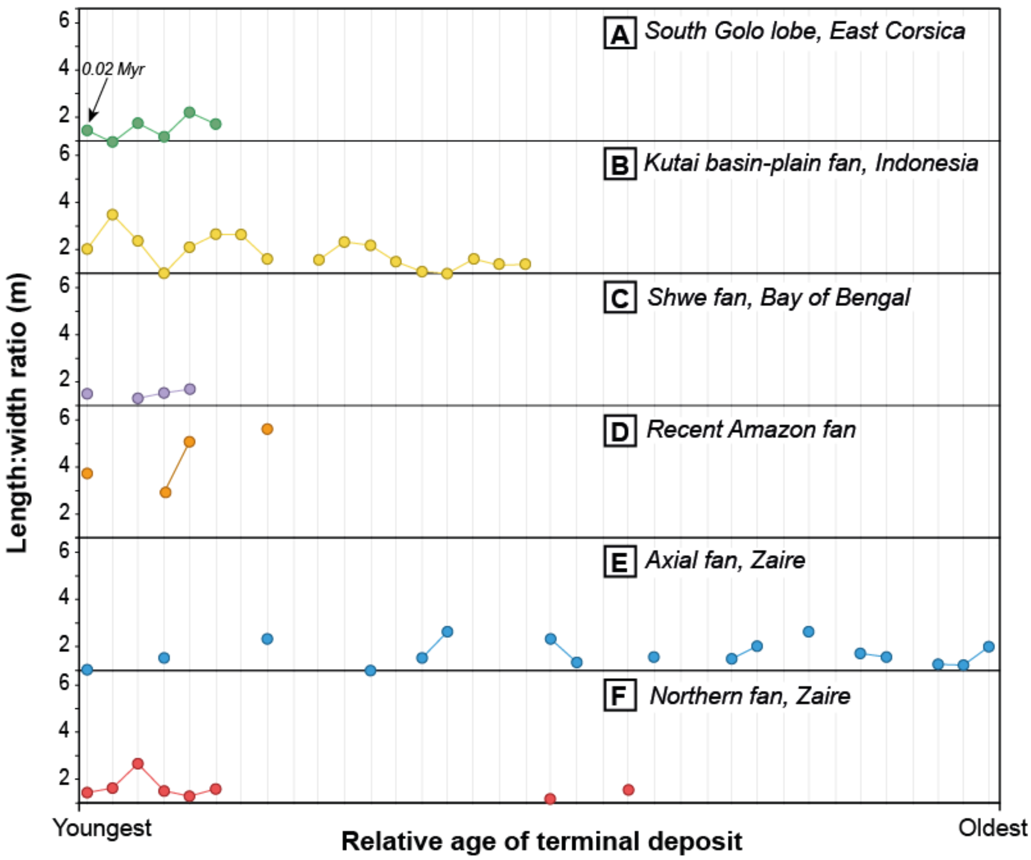

Fig. 11. Changes in lobate terminal deposit length-to-width ratios (vertical axes), over relative time scales (horizontal axis). Each box corresponds to a different subset, where terminal deposits are either i) contained in a larger parent terminal deposit (i.e., the South Golo fan, Kutai fan and Shwe fan) or ii) are the largest known lobate terminal deposits on the basin-floor in the entire fan (i.e., the Amazon and Zaire deposits). For each subset, the comparison only includes 'true' widths and lengths of deposits of the same hierarchical order. Each point reflects a terminal deposit; lines are broken where intervening deposits exist but suitable data on their dimensions are lacking. Total duration of deposition for each subset is typically over 10^4 yr timescales, except for the Zaire (10^5 yr); the time scale is unknown for the Shwe fan. Absolute age is shown for the youngest terminal deposit of the South Golo lobe (A).

3.5 Synthetic facies models

Synthetic facies models that account for the proportion of deposits of different types and for trends and distributions in lithologies can be built at a variety of geological scales, i.e., for bed, element or depositional environments. Figure 12 shows the relative proportion of sedimentary structures found in the sandstone intervals of different element types. Output on the proportion of sedimentary units can be generated based on the synthesis of data from many elements, and with consideration of biases related to variations in size and representativeness of the available samples. For example, in Fig. 12 facies proportions are presented based on both (i) scaled averages that assign equal weight to each element to account for sampling biases (darker), and (ii) the total sum of their thickness (lighter).

Facies models can be tailored to specific environmental scenarios, e.g., system parameters, architectural or facies characteristics, bed relationships, or position in a sub-environment. For example, Fig. 13 compares the grain size and sedimentary structures of the sandstone intervals found in channel-related detailed element types (see Table 3) associated with sandy systems. Similar proportional grain-size and sedimentary structure trends can be identified for both lateral accretion packages (LAPs) and aggradational channel fills. For example, over 50% of the classified facies units for both element types are 'massive'. LAPs are seen to contain a higher proportion of gravel, as well as of cross-stratification compared to aggradational channel fills (Fig. 13). This trend is also identified when considering only systems that include data for both LAPs and aggradational channel fills. In these systems, the total proportion of gravel is equal to 47% in LAPs (N = 1224 facies, 10 elements), compared to 36% in aggradational channel fills (N = 1061 facies, 30 elements), whereas the proportion of cross-stratified sands is equal to 17% in LAPs (N = 791 facies, 10 elements), compared to 6% (N= 547 facies, 23 elements). As new data is added to the database and the sample size is increased, further investigation can take place to verify the statistical significance of these results, as well as use them to analyse experimental or numerical process models. Quantified facies models of this type can also be used as 'synthetic analogues' for interpretations and predictions in subsurface studies.

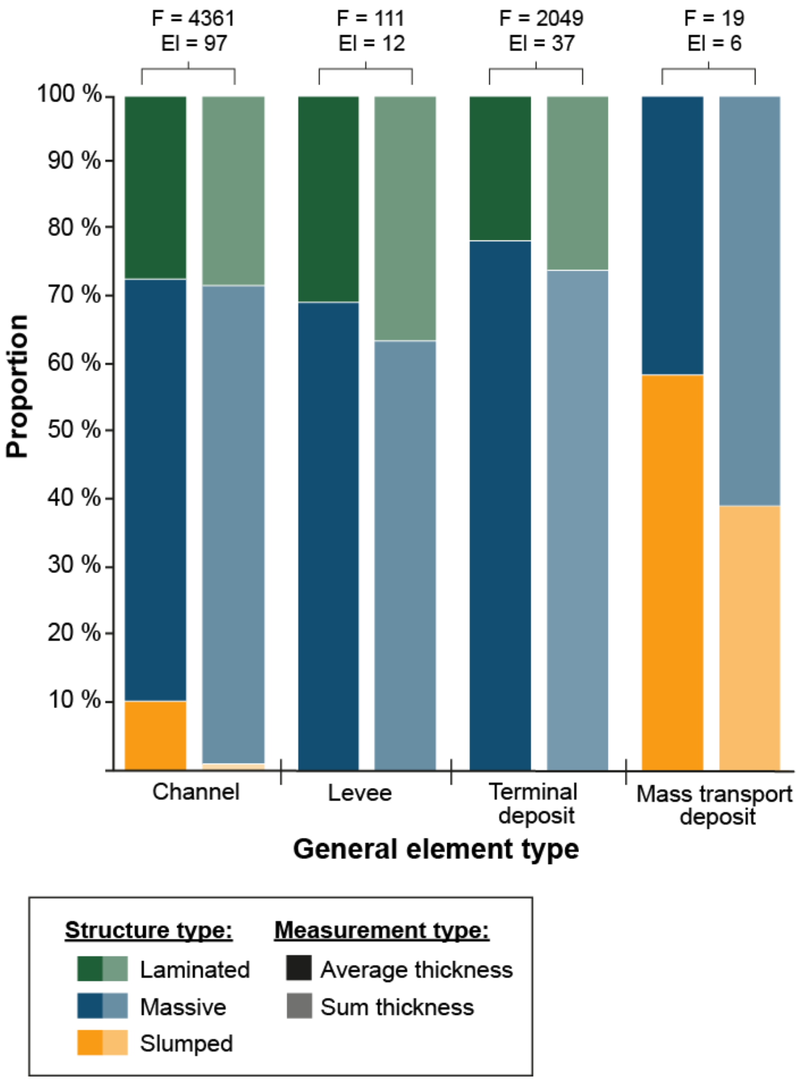

Fig. 12. Bar chart showing the different sedimentary structures found in sandstone intervals observed in different general element types (see Table 2 for element type descriptions). Two different proportional measures are shown: i) scaled averages of proportions, where each element is given an equal weight (darker bars) and ii) proportions based on the total sum of facies thickness in all elements (lighter bars). F = number of facies, El = number of elements.

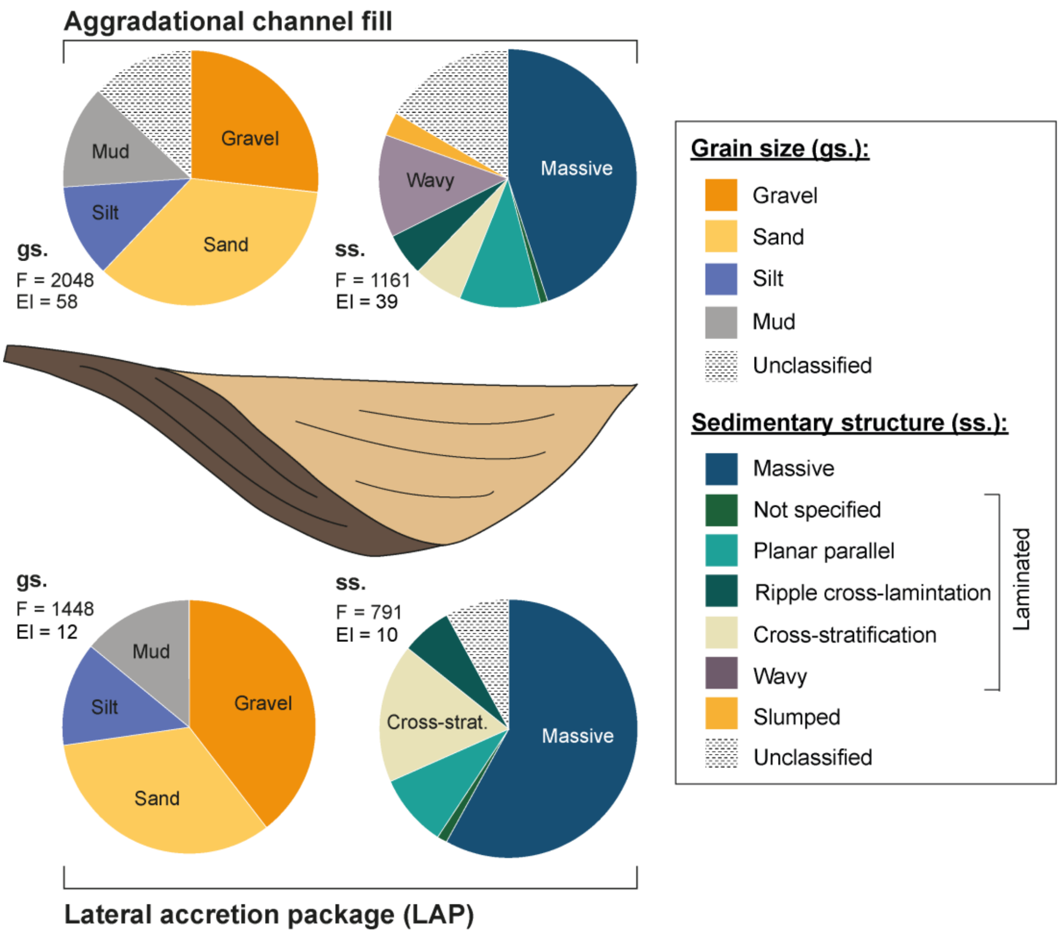

Fig. 13. Facies proportion models for deep-marine channel-related architecture. Scaled average proportions based on facies thicknesses are shown for grain size (gs.) and sedimentary structure, including lamination types from sand/sandstone facies (ss.). Note that the drawing is for illustration only and it does not imply that the element proportions shown are based upon spatial relations. F = number of facies, El = number of elements.

3.6 Vertical organisation of facies

Quantitative descriptions of the vertical distribution of facies can be built using facies transitions and 1D facies ordering information stored in DMAKS. For instance, Fig. 14 shows high probability (>60%) for fining upwards grain size trends in sandstones and gravels in channel elements of sandy systems. Silty facies, however, are more likely to transition upwards to coarser fractions, suggesting that complete fining upwards sequences are rarely deposited or preserved in the considered dataset. Such outputs on quantitative facies analysis can be used to inform stochastic facies models (e.g., Markov chain analysis), similar to the deep-marine facies studies of Falivene et al. (2006) and Li et al. (2018).

The recurrence of specific facies trends in beds can also be investigated. For example, Fig. 15 depicts facies trends identified in the San Clemente slope channel-system case study (Capistrano Formation, Li et al., 2016). The modelling of facies distribution within beds can be used to improve characterisation of reservoir quality at the bed scale. Facies distributions can also be used to model the cyclicity of depositional patterns, which in turn can be used to inform geological modelling efforts. For instance, DMAKS could be used to evaluate, statistically, the occurrence and distribution of facies as represented in proposed facies models (e.g., in the classification of hybrid event beds; Haughton et al., 2009; Fonnesu et al., 2018); such approaches would help inform process interpretations via the analysis of large sets of standardised data.

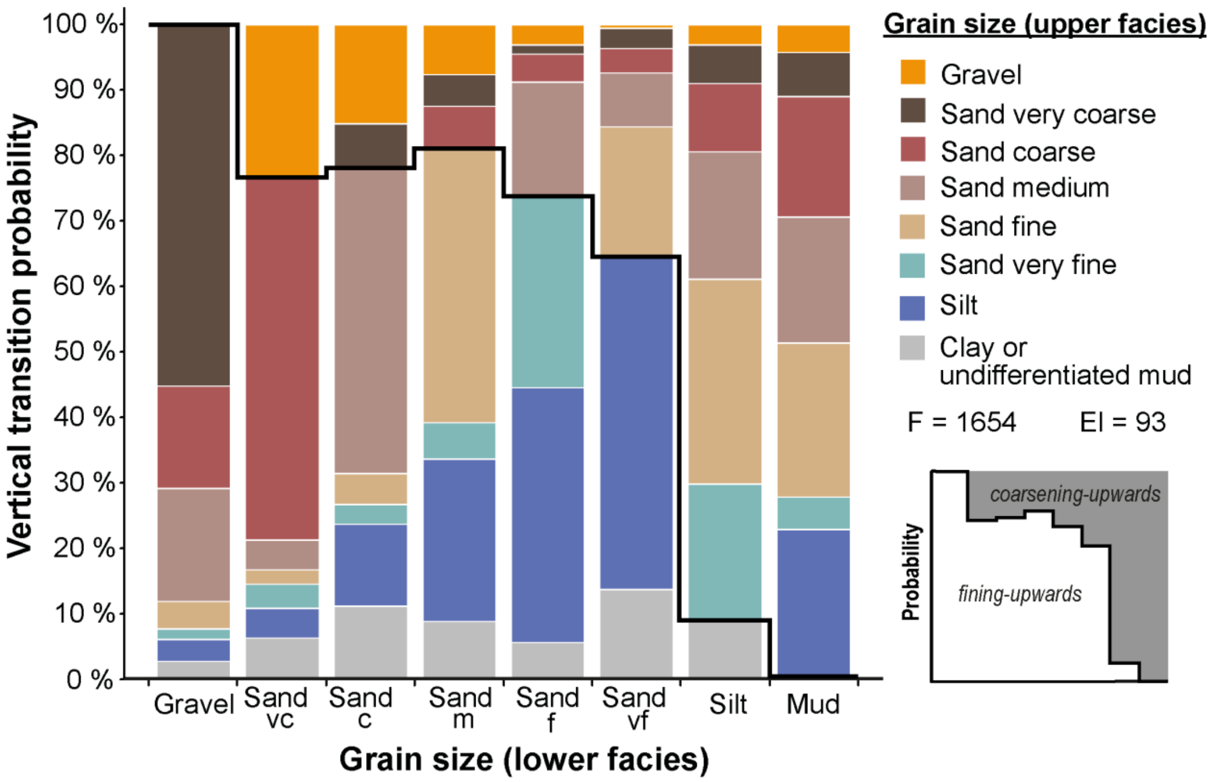

Fig. 14. Vertical transition probability for grain-size classes of in-channel facies units, from the starting (lower) facies type indicated on the horizontal axis. Transitions between facies of the same grain size are not included. Only facies from channel elements in sandy systems are considered. The vertical transition grain size classes are presented in a manner whereby coarser classes are at the top. A continuous black line marks the position of the grain size of the lower facies and therefore facies transitions counts above the line indicate a transition to coarser sediments (coarsening-upward), while facies transition counts below the line show the probability of vertically passing to a finer sediment (fining-upward), see illustration in bottom-right corner. F = number of facies, El = number of elements.

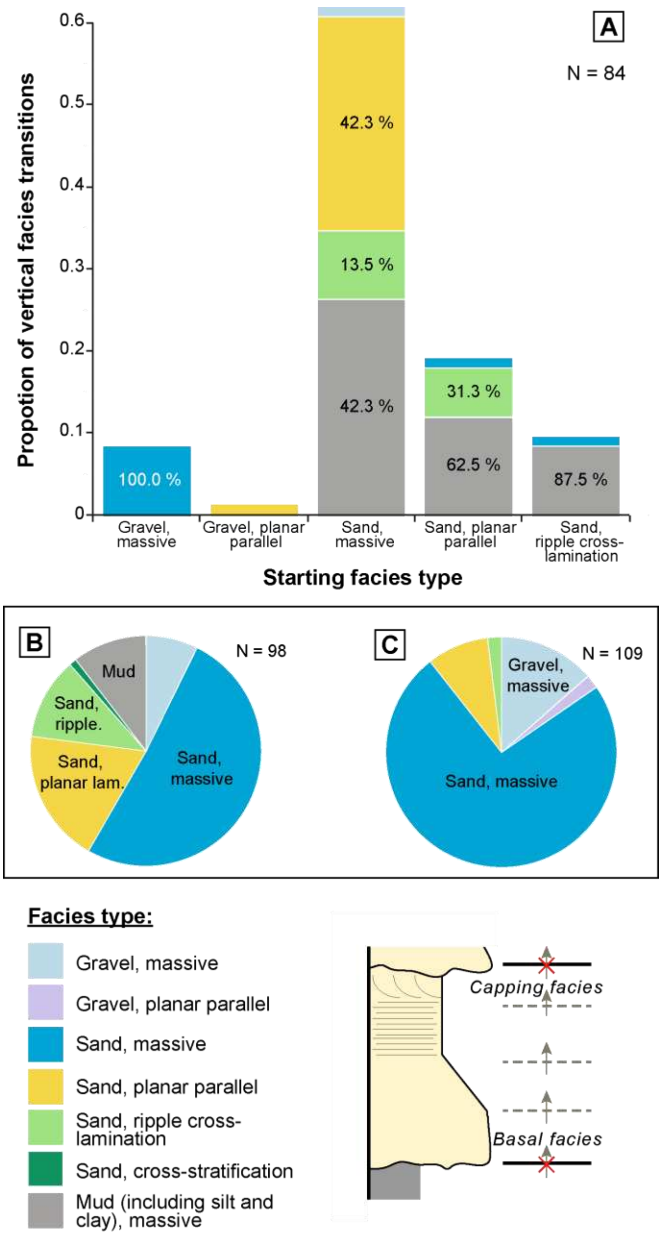

Fig. 15. Facies proportions derived from beds contained in channel deposits of the San Clemente case study (Li et al., 2016; Table 1). A) Facies-type vertical transitions contained in units described as beds in the original source. Transitions across bedding surfaces are excluded (see illustration in key). X-axis categories represent the lower facies and colours represent the upper facies. Capping (B) and basal (C) facies-type proportions calculated based upon their sum thickness. Only beds containing more than one facies are included in B, while C also includes beds with only one facies. Facies types are classified based upon grain size, sedimentary structures and lamination type, if applicable.

3.7 Net-to-gross ratios

Outputs on the proportion of facies in specific types of elements can be used to calculate sandstone proportions or net-to-gross ratios, and the variability in these values can be quantified through consideration of multiple elements. For example, Fig. 16 shows the distribution in the proportion of sand observed in different element types. Net-to-gross values can be tailored to user-defined ‘net’ specifications and obtained by filtering data based on the attributes on which the systems are classified, to enable consideration of relevant analogues. For instance, Fig. 17 considers only channels found on the slope and in sandy systems (i.e., in which the dominant grain size was reported as mixed or sand-rich in the original sources). Metrics of this type can inform predictions relating to total reservoir volume and, when paired with information on spatial variations in lithological heterogeneity (e.g., transition data, or position classifiers), its distribution. For example, Fig. 17 depicts a base case for the decrease in net-to-gross ratio seen from the axis of channel elements to their margin – supporting the slope models of Richards & Bowman (1998) and Hubbard et al. (2014), as well as the outcrop studies of Campion et al. (2000; Capistrano Formation) and Macauley & Hubbard (2013; Tres Pasos Formation). The ability to link facies records (and their bed bounding-surface relationships; demonstrated in Section 3.6) to a position within their sub-environment could further be used to characterise likely process-product relationships.

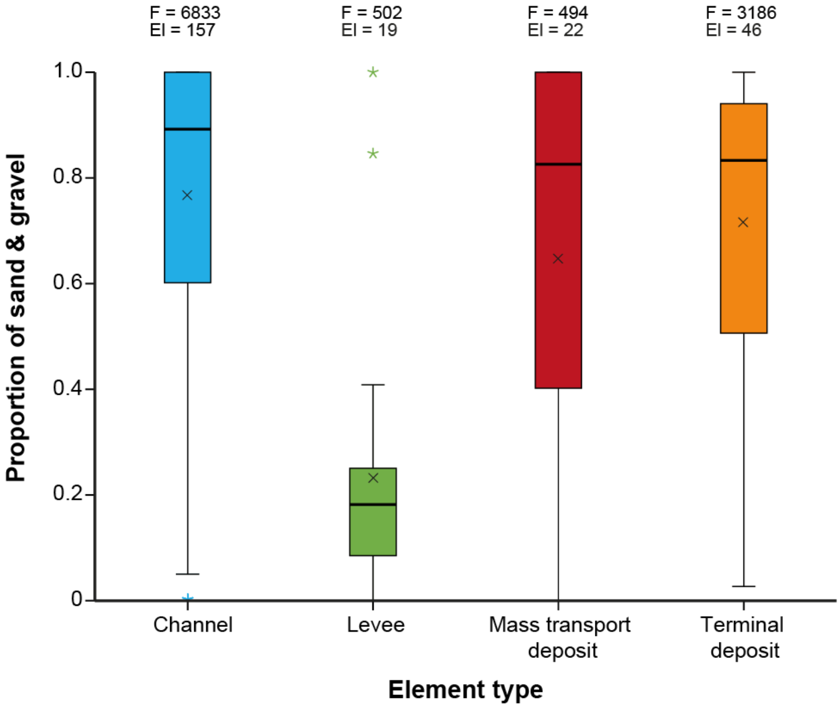

Fig. 16. Proportion of sand and gravel found in different element types. Proportions are calculated based on the thickness of sandstone and conglomerate intervals divided by the full thickness of each element. A facies may be counted more than once if contained in elements that are organised hierarchically. Each box represents the interquartile range and includes a median line. Crosses show mean values; stars denote outliers. F = number of facies; EI = number of elements.

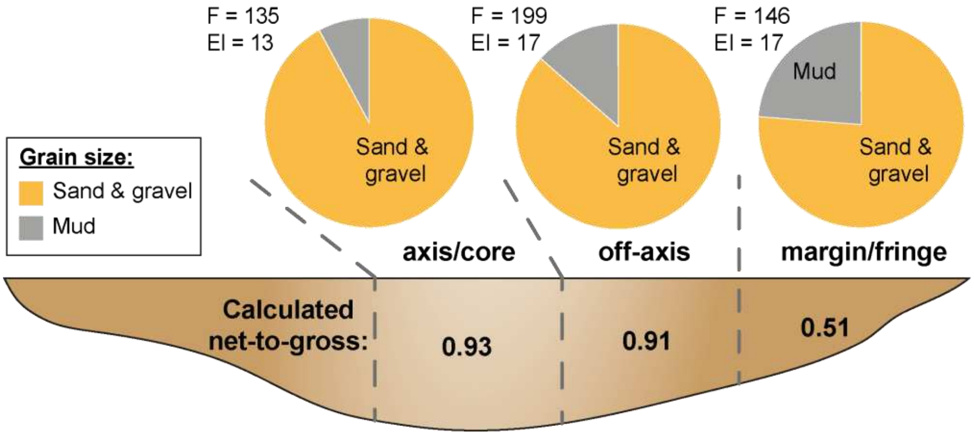

Fig. 17. Relative proportion of sand and gravel vs mud specified by lateral position in channel elements. Proportions calculated by averaging the sum of the thicknesses of a grain size against each facies sequences total vertical thickness. Only facies descriptions with a DQI rating of ‘A’ or ‘B’ have been considered. ‘Mud’ includes silt and clay. Data are filtered to include only slope channels found in dominantly sandy systems. F = number of facies; EI = number of elements.

4. Discussion

DMAKS enables the effective integration of data from the modern seafloor, ancient subsurface and outcropping deep-marine successions, facilitating a comprehensive characterisation and comparison of deep-marine systems (e.g., Fig. 6 A and B; Slatt, 2000; Gamberi et al., 2013). The scope of this databasing effort is deliberately wide, aiming to cover both the broad range of environmental settings found in deep-marine systems, together with associated hierarchical and spatial relationships between and within geological entities; this breadth of scope distinguishes it from other approaches (e.g., Cossey & Associates Inc., 2004; Baas et al., 2005; Moscardelli & Wood, 2015; Clare et al., 2018). DMAKS facilitates the characterisation of deep-marine systems by producing quantitative information on the geometries, spatial arrangements and lithological organization of modern landforms and preserved deposits, which can be derived from single or multiple case studies. It can therefore be used to conduct fundamental research, based upon meta-analysis and synthesis of legacy data, or be employed as a resource in subsurface applications that benefit from quantification of sedimentological properties. DMAKS demonstrates the benefits of data standardisation in deep-marine sedimentology, as data integration from multiple sources improves the significance of statistical outputs. The wide range of geological parameters considered allows data to be filtered by multiple variables, to produce outputs that are relevant to specific academic research questions or that can act as synthetic analogues to particular hydrocarbon reservoirs. Through quantification of intra- and inter-system variability in sedimentary architecture, DMAKS enables the geological uncertainties affecting subsurface workflows to be accounted for, and to some extent, reduced.

The database is designed to be refined and extended, in response to scientific progress in the field of deep-marine sedimentology. It complements existing databases for fluvial (Colombera et al., 2012) and paralic and shallow-marine depositional systems (Colombera et al., 2016); a longer-term goal is database integration, to facilitate linked analysis of sedimentary architectures across a range of connected clastic environments.

5. Summary

DMAKS is a database storing field- and literature-derived standardised sedimentological data pertaining to siliciclastic deep-marine depositional systems. DMAKS integrates data from multiple studies, and considers the geometry, spatial and hierarchical arrangements, and internal facies properties of deposits and landforms, assigned to systems and case studies classified on boundary conditions, descriptions of the context of deposition, and other metadata. DMAKS can be queried flexibly to produce quantitative outputs that can be used to (i) undertake quantitative comparative analyses between multiple studies and to (ii) produce syntheses of datasets that act as quantitative facies models or composite analogues. DMAKS finds application in both pure and applied research, particularly for testing process-product relationships via a meta-analytical approach, and for enabling subsurface predictions that are realistic and effectively account for geological uncertainty.

Acknowledgments

We thank Amandine Prélat and an anonymous reviewer for their constructive comments, which have improved the paper. NERC (Follow-on Fund award NE/P01691X/1) and the sponsors of the Turbidites Research Group, University of Leeds (AkerBP, Anadarko, BP, ConocoPhillips, Dana, Equinor, ENI, HESS, Murphy, Nexen, OMV, Petronas, Shell, Tullow and Woodside) are thanked for financial support.

References

Albouy, E., Deschamps, R., Euzen, T. & Eschard, R., 2007. Stratigraphic architecture of a channel complex in the canyon-mouth setting of the Lower Pab Basin-Floor Fan, Drabber Dhora, Pakistan. In: Nilsen, T. H., Shew, R. D., Steffens, G. S. and Studlick, J. R. J. (Eds). Atlas of Deep-Water Outcrops. AAPG Studies in Geology, 56, p. 295-298.

Arbues, P., Mellere, D., Falivene, O., Fernández, O., Munoz, J. A., Marzo, M. & de Gibert, J. M., 2007. Context and Architecture of the Ainsa-1-Quarry Channel Complex, Spain. In: Nilsen, T. H., Shew, R. D., Steffens, G. S. & Studlick, J. R. J. (Eds). Atlas of Deep-Water Outcrops, CD-ROM. AAPG Studies in Geology, 56, p. 1-20.

Armitage, D. A., Romans, B. W., Covault, J. A. & Graham, S. A., 2009. The Influence of Mass-Transport-Deposit Surface Topography on the Evolution of Turbidite Architecture: the Sierra Contreras, Tres Pasos Formation (Cretaceous), Southern Chile. Journal of Sedimentary Research, 79, (5-6), p. 287-301.

Arnot, M. J., Browne, G. H. & King, P. R., 2007(a). Thick-bedded sandstone facies in a middle basin-floor fan setting, Mount Messenger Formation, Mohakatino Beach, New Zealand. In: Nilsen, T. H., Shew, R. D., Steffens, G. S. & Studlick, J. R. J. (Eds). Atlas of Deep-Water Outcrops. AAPG Studies in Geology, 56, p. 241-244.

Arnot, M. J., King, P. R., Browne, G. H. & Helle, K., 2007(b). Channelized, Innermost, Basin-Floor-Fan Morphologies, Mount Messenger Formation, Waikiekie South Beach and Inland, New Zealand. In: Nilsen, T. H., Shew, R. D., Steffens, G. S. & Studlick, J. R. J. (Eds). Atlas of Deep-Water Outcrops. AAPG Studies in Geology, 56, p. 249-256.

Arnott, R. W. C., 2007(a). Architecture of lateral-accretion deposits in two stacked, deep-water, sinuous channel fills: relationship between coarse channel-fill and adjacent inner-bend leveee deposits, Isaac Channel 2, Castle Creek South, Windermere Supergroup, British Columbia, Canada. In: Nilsen, T. H., Shew, R. D., Steffens, G. S. and Studlick, J. R. J. (Eds). Atlas of Deep-Water Outcrops. AAPG Studies in Geology, 56, p. 89-92.

Arnott, R. W. C., 2007(b). Stratal architecture and origin of lateral accretion deposits (LADs) and conterminuous inner-bank levee deposits in a base-of-slope sinuous channel, lower Isaac Formation (Neoproterozoic), East-Central British Columbia, Canada. Marine and Petroleum Geology, 24, p. 515-528.

Arnott, R. W. C. & Ross, G. M., 2007. Overview: Outcrop Analysis of an Ancient, Passive Margin, Turbidite System: Windermere Supergroup, British Columbia, Canada. In: Nilsen, T. H., Shew, R. D., Steffens, G. S. & Studlick, J. R. J. (Eds). Atlas of Deep-Water Outcrops. AAPG Studies in Geology, 56, p. 81-84.

Baas, J.H., McCaffrey, W.D. & Knipe, R.J., 2005. The Deep-Water Architecture Knowledge Base: towards an objective comparison of deep-marine sedimentary systems. Petroleum Geoscience, 11, p. 309-320.

Babonneau, N., Savoye, B., Cremer, M. & Klein, B., 2002. Morphology and architecture of the present canyon and channel system of the Zaire deep-sea fan. Marine and Petroleum Geology, 19, (4), p. 445-467.

Babonneau, N., Savoye, B., Cremer, M. & Bez, M., 2010. Sedimentary architecture in meanders of a submarine channel; detailed study of the present Congo turbidite channel (Zaiango Project). Journal of Sedimentary Research, 80, (9-10), p. 852-866.

Barnes, N. E. & Normark, W. R., 1985. Diagnostic parameters for comparing modern submarine fans and ancient turbidite systems. In: Bouma, A. H., Normark, W. R. & Barnes, N. E. (Eds). Submarine Fans and Related Turbidite Systems, p. 13-14.

Barton, M. D. & Dutton, S. P., 2007. A sand-rich, basin-floor turbidite system, Willow Mountain, Texas, USA. In: Nilsen, T. H., Shew, R. D., Steffens, G. S. and Studlick, J. R. J. (Eds). Atlas of Deep-Water Outcrops. AAPG Studies in Geology, 56, p. 418-421.

Barton, M. D., O'Byrne, C. J., Steffens, G. S., Pirmez, C. & Buergisser, H., 2007(a). Architecture of an aggradational deep-water channel complex: Channel Complex 2, Isaac Formation, Windermere Supergroup, British Columbia, Canada. In: Nilsen, T. H., Shew, R. D., Steffens, G. S. and Studlick, J. R. J. (Eds). Atlas of Deep-Water Outcrops. AAPG Studies in Geology, 56, p. 106-110.

Barton, M. D., Craig, P., Prather, B. E. & Copus, J., 2007(b). Facies architecture of channel-levee deposits, Lago Nordenskjold and Laguna Mellizas Sur, Cerro Toro Formation, Chile. In: Nilsen, T. H., Shew, R. D., Steffens, G. S. and Studlick, J. R. J. (Eds). Atlas of Deep-Water Outcrops. AAPG Studies in Geology, 56, p. 157-161.

Barton, M. D., Steffens, G. S. & O'Byrne, C. J., 2007(c). Facies architecture of a submarine-slope channel complex, Condor West Channel, Cerro Toro Formation, Chile. In: Nilsen, T. H., Shew, R. D., Steffens, G. S. and Studlick, J. R. J. (Eds). Atlas of Deep-Water Outcrops. AAPG Studies in Geology, 56, p. 149-153.

Bayliss, N. J. & Pickering, K. T., 2015. Transition from deep-marine lower-slope erosional channels to proximal basin-floor stacked channel-levee-overbank deposits, and syn-sedimentary growth structures, Middle Eocene Banaston System, Ainsa Basin, Spanish Pyrenees. Earth-Science Reviews, 144, p. 23-46.

Beaubouef, R. T., Rossen, C., Zelt, F. B., Sullivan, M. D., Mohrig, D. C. & Jennette, D. C., 1999. Deep-Water Sandstones, Brushy Canyon Formation, West Texas. The American Association of Petroleum Geologists.

Beaubouef, R. T., Rossen, C. & Lovell, R. W. W., 2007. The Beacon Channel: a newly recognized architectural type in the Brushy Canyon Formation, Texas, USA. In: Nilsen, T. H., Shew, R. D., Steffens, G. S. & Studlick, J. R. J. (Eds). Atlas of Deep-Water Outcrops. AAPG Studies in Geology, 56, p. 432-443.

Bouma, A. H., 1982. Intraslope basins in Northwest Gulf of Mexico; a key to ancient submarine canyons and fans. In: Watkins, J. S. and Drake, C. L. (Eds). Studies in continental margin geology. AAPG Memoir, Tulsa, OK, United States, American Association of Petroleum Geologists, 34, p. 567-581.

Bouma, A. H. & Delery, A. M., 2007. Fine-grained Permian Turbidites of Southwestern South Africa: Tanqua Karoo and Laingsburg Deep-water Basins. In: Nilsen, T. H., Shew, R. D., Steffens, G. S. & Studlick, J. R. J. (Eds). Atlas of Deep-Water Outcrops, CD-ROM. AAPG Studies in Geology, 56, pp. 1-19.

Bouma, A. H., Delery, A. M. & Scott, E. D., 2007. Introduction to Deep-water Deposits of the Tanqua Karoo, South Africa. In: Nilsen, T. H., Shew, R. D., Steffens, G. S. & Studlick, J. R. J. (Eds). Atlas of Deep-Water Outcrops. AAPG Studies in Geology, 56, pp. 302-304.

Bourget, J., Zaragosi, S., Mulder, T., Schneider, J. L., Garlan, T., Van Toer, A., Mas, V. & Ellouz-Zimmermann, N., 2010. Hyperpycnal-fed turbidite lobe architecture and recent sedimentary processes: A case study from the Al Batha turbidite system, Oman margin. Sedimentary Geology, 229, (3), p. 144-159.

Browne, G. H., Slatt, R. M. & King, P. R., 2000. Contrasting Styles of Basin-Floor Fan and Slope Fan Deposition: Mount Messenger Formation, New Zealand. In: Bouma, A. H. and Stone, C. G. (Eds). Fine-grained turbidite systems. AAPG Memoir 72/SEPM Special Publication, 68, p. 143-152.

Browne, G. H., King, P. R., Higgs, K. E. & Slatt, R. M., 2005. Grain-size characteristics for distinguishing basin floor fan and slope fan depositional settings: outcrop and subsurface examples from the late Miocene Mount Messenger Formation, New Zealand. New Zealand Journal of Geology and Geophysics, 48, (2), p. 213-227.

Browne, G. H., King, P. R., Arnot, M. J. & Helle, K., 2007(a). A complete middle-to-inner basin-floor-fan cycle, Mount Messenger Formation, Tongaporutu, New Zealand. In: Nilsen, T. H., Shew, R. D., Steffens, G. S. and Studlick, J. R. J. (Eds). Atlas of Deep-Water Outcrops. AAPG Studies in Geology, 56, p. 245-248.

Browne, G. H., King, P. R., Arnot, M. J. & Slatt, R. M., 2007(b). Architecture of base-of-slope fans, Mount Messenger Formation, Pukearuhe Beach, New Zealand. In: Nilsen, T. H., Shew, R. D., Steffens, G. S. & Studlick, J. R. J. (Eds). Atlas of Deep-Water Outcrops. AAPG Studies in Geology, 56, p. 257-261.

Brunt, R.L., 2003. Vertical transitions in turbidite facies and sedimentary architecture: insights from the Grès du Champsaur, SE France, and from laboratory experiments. Doctoral Thesis, University of Leeds.

Brunt, R. L. & McCaffrey, W. D., 2007. Heterogeneity of fill within an incised channel: The Oligocene Gres du Champsaur, SE France. Marine and Petroleum Geology, 24, p. 529-539.

Brunt, R. L., McCaffrey, W. D. & Butler, R. W. H., 2007. Setting and architectural elements of the Champsaur Sandstones, France. In: Nilsen, T. H., Shew, R. D., Steffens, G. S. & Studlick, J. R. J. (Eds). Atlas of Deep-Water Outcrops. AAPG Studies in Geology, 56, p. 188-191.

Brunt, R. L., Hodgson, D. M., Flint, S. S., Pringle, J. K., Di Celma, C. N., Prelat, A. & Grecula, M., 2013. Confined to unconfined: Anatomy of a base of slope succession, Karoo Basin, South Africa. Marine and Petroleum Geology, 41, p. 206-221.

Butterworth, P. J., Crame, J. A., Howlett, P. J. & Macdonald, D. I. M., 1988. Lithostratigraphy of Upper Jurassic-Lower Cretaceous strata of eastern Alexander Island, Antarctica. Cretaceous Research, 9, (3), p. 249-264.

Butterworth, P. J. & MacDonald, D. I. M., 2007. Channel-levee complexes of the Fossil Bluff Group, Antarctica. In: Nilsen, T. H., Shew, R. D., Steffens, G. S. and Studlick, J. R. J. (Eds). Atlas of Deep-Water Outcrops. AAPG Studies in Geology, 56, p. 36-41.

Callow, R. H. T., McIlroy, D., Kneller, B. & Dykstra, M., 2013(a). Ichnology of Late Cretaceous Turbidites from the Rosario Formation, Baja California, Mexico. Ichnos-an International Journal for Plant and Animal Traces, 20, (1), p. 1-14.

Callow, R. H. T., McIlroy, D., Kneller, B. C. & Dykstra, M., 2013(b). Integrated ichnological and sedimentological analysis of a Late Cretaceous submarine channel-levee system: The Rosario Formation, Baja California, Mexico. Marine and Petroleum Geology, 41, p. 277-294.

Campion, K. M., Sprague, A. R., Mohrig, D., Lovell, R. W., Drzewiecki, P. A., Sullivan, M. D., Ardill, J. A., Jensen, G. N. & Sickafoose, D. K., 2000. Outcrop Expression of Confined Channel Complexes. In: GCSSEPM Foundation 20th Annual Research Conference, Deep-Water Reservoirs of the World, p. 127-151.

Campbell, C.V., 1967. Lamina, Laminaset, Bed and Bedset. Sedimentology, 8, p. 7-26.

Clare, M., Chaytor, J., Dabson, O., Gamboa, D., Georgiopoulou, A., Eady, H., Hunt, J., Jackson, C., Katz, O., Krastel, S., León, R., Micallef, A., Moernaut, J., Moriconi, R., Moscardelli, L., Mueller, C., Normandeau, A., Patacci, M., Steventon, M., Urlaub, M., Völker D., Wood, L. & Jobe, Z., 2018. A consistent global approach for the morphometric characterization of subaqueous landslides. Geological society, London, Special Publications, 477.

Clark, J. D. and Pickering, K.T., 1996. Submarine channels. Processes and architecture. Vallis Press, London.

Colombera, L., Mountney, N.P. & McCaffrey, W.D., 2012. A relational database for the digitisation of fluvial architecture: concepts and example applications. Petroleum Geoscience, 18, p. 129-140.

Colombera, L., Mountney, N.P. & McCaffrey, W.D., 2015. A meta-study of relationships between fluvial channel-body stacking pattern and aggradation rate: Implications for sequence stratigraphy. Geology, 43, (4), p. 283–286.

Colombera, L., Mountney, N.P., Hodgson, D.M., & McCaffrey, W.D., 2016. The Shallow-Marine Architecture Knowledge Store: A database for the characterization of shallow-marine and paralic depositional systems. Marine and Petroleum Geology, 75, p. 83-99.

Cossey, S.P.J., 2005. Turbidite databases [online]. Available at: http://cosseygeo.com/databases/databases.htm [Accessed 12/06/2018]

Crevello, P. D., Johnson, H. D., Tongkul, F. & Wells, M. R., 2007(a). Overview of Mixed Braided- and Leveed-channel Turbidites, West Crocker Fan System, Northwest Borneo. In: Nilsen, T. H., Shew, R. D., Steffens, G. S. & Studlick, J. R. J. (Eds). Atlas of Deep-Water Outcrops. AAPG Studies in Geology, 56, p. 50-52.

Crevello, P. D., Johnson, H. D., Tongkul, F. & Wells, M. R., 2007(b). Lobe and channel deposits, Papar Highway, Northwest Borneo. In: Nilsen, T. H., Shew, R. D., Steffens, G. S. & Studlick, J. R. J. (Eds). Atlas of Deep-Water Outcrops. AAPG Studies in Geology, 56, p. 67-69.

Crevello, P. D., Johnson, H. D., Tongkul, F. & Wells, M. R., 2007(c). Mixed Braided and Leveed-channel Turbidites, West Crocker Fan System, Northwest Borneo. In: Nilsen, T. H., Shew, R. D., Steffens, G. S. & Studlick, J. R. J. (Eds). Atlas of Deep-Water Outcrops, CD-ROM. AAPG Studies in Geology, 56, p. 1-32.

Cullis, S., Colombera, L., Patacci, M. & McCaffrey, W.D., 2018. Hierarchical classifications of the sedimentary architecture of deep-marine depositional systems. Earth-Science Reviews, 179, p. 38-71.

Damuth, J. E., 1994. Neogene gravity tectonics and depositional processes on the deep Niger Delta continental margin. Marine and Petroleum Geology, 11, (3), p. 320-346.

Delery, A. M. & Bouma, A. H., 2003. Aspect ratios of coarse-grained and fine-grained submarine fan channels. Transactions - Gulf Coast Association of Geological Societies, 53, p. 170-182.

Dennielou, B., Droz, L., Babonneau, N., Jacq, C., Bonnel, C., Picot, M., Le Saout, M., Saout, Y., Bez, M., Savoye, B., Olu, K. & Rabouille, C., 2017. Morphology, structure, composition and build-up processes of the active channel-mouth lobe complex of the Congo deep-sea fan with inputs from remotely operated underwater vehicle (ROV) multibeam and video surveys. Deep-Sea Research Part II-Topical Studies in Oceanography, 142, pp. 25-49.

Deptuck, M. E., Sylvester, Z., Pirmez, C. & O'Byrne, C., 2007. Migration-aggradation history and 3-D seismic geomorphology of submarine channels in the Pleistocene Benin-major Canyon, western Niger Delta slope. Marine and Petroleum Geology, 24, p. 406-433.

Deptuck, M. E., Piper, D. J. W., Savoye, B. & Gervais, A., 2008. Dimensions and architecture of late Pleistocene submarine lobes off the northern margin of East Corsica. Sedimentology, 55, (4), p. 869-898.

Deptuck, M. E., Sylvester, Z. & O'Byrne, C., 2012. Pleistocene seascape evolution above a 'simple' stepped slope - western Niger delta. In: Prather, B. E., Deptuck, M. E., Mohrig, D., Van Hoorn, B. & Wynn, R. B. (Eds). Application of the Principles of Seismic Geomorphology to Continental-Slope and Base-of-Slope Systems: Case Studies from Seafloor and Near-Seafloor Analogues. SEPM Special Publication, 99, p. 199-222.

Di Celma, C. N., Brunt, R. L., Hodgson, D. M., Flint, S. S. & Kavanagh, J. P., 2011. Spatial and Temporal Evolution of a Permian Submarine Slope Channel-Levee System, Karoo Basin, South Africa. Journal of Sedimentary Research, 81 (7-8), pp. 579-599.

Di Celma, C., Teloni, R. & Rustichelli, A., 2014. Large-scale stratigraphic architecture and sequence analysis of an early Pleistocene submarine canyon fill, Monte Ascensione succession (Peri-Adriatic basin, eastern central Italy). International Journal of Earth Sciences, 103, (3), p. 843-875.

Droz, L., Marsset, T., Ondreas, H., Lopez, M., Savoye, B. & Spy-Anderson, F.-L., 2003. Architecture of an active mud-rich turbidite system; the Zaire Fan (Congo-Angola margin Southeast Atlantic); results from ZaiAngo 1 and 2 cruises. AAPG Bulletin, 87, (7), p. 1145-1168.

Dykstra, M. & Kneller, B. C., 2007. Canyon San Fernando, Baja California, Mexico: A deep-water channel-levee complex that evolved from submarine canyon confinement to unconfined deposition. In: Nilsen, T. H., Shew, R. D., Steffens, G. S. & Studlick, J. R. J. (Eds). Atlas of Deep-Water Outcrops, CD-ROM. AAPG Studies in Geology, 56, p. 1-14.

Euzen, T., Eschard, R. & Albouy, E., 2007(a). Stratigraphic architecture of a channel complex in the midfan setting of the Lower Pab Basin Floor Fan, North Baddho Dhora, Pakistan. In: Nilsen, T. H., Shew, R. D., Steffens, G. S. and Studlick, J. R. J. (Eds). Atlas of Deep-Water Outcrops. AAPG Studies in Geology, 56, p. 290-294.

Euzen, T., Eschard, R., Albouy, E. & Deschamps, R., 2007(b). Reservoir Architecture of a Turbidite Channel Complex in the Pab Formation, Pakistan. In: Nilsen, T. H., Shew, R. D., Steffens, G. S. and Studlick, J. R. J. (Eds). Atlas of Deep-Water Outcrops, CD-ROM. AAPG Studies in Geology, 56, p. 1-20.

Eschard, R., Albouy, E., Gaumet, F. & Ayub, A., 2004. Comparing the depositional architecture of basin floor fans and slope fans in the Pab Sandstone, Maastrichtian, Pakistan. In: Lomas, S. A. & Joseph, P. (Eds). Confined Turbidite Systems. Geological Society of London Special Publication, 222, p. 159-185.

Falivene, O., Arbues, P., Gardiner, A., Pickup, G., Munoz, J. A. & Cabrera, L., 2006. Best practice stochastic facies modeling from a channel-fill turbidite sandstone analog (the Quarry outcrop, Eocene Ainsa basin, northeast Spain). AAPG Bulletin, 90, (7), p. 1003-1029.

Falivene, O., Arbues, P., Ledo, J., Benjumea, B., Munoz, J. A., Fernandez, O. & Martinez, S., 2010. Synthetic seismic models from outcrop-derived reservoir-scale three-dimensional facies models: The Eocene Ainsa turbidite system (southern Pyrenees). AAPG Bulletin, 94, (3), p. 317-343.

Fildani, A., Drinkwater, N. J., Weislogel, A., McHargue, T., Hodgson, D. M. & Flint, S. S., 2007. Age controls on the Tanqua and Laingsburg deep-water systems: New insights on the evolution and sedimentary fill of the Karoo basin, South Africa. Journal of Sedimentary Research, 77, pp. 901-908.

Flint, S. S., Hodgson, D. M., Sprague, A. R., Brunt, R. L., van der Merwe, W. C., Figueiredo, J. J. P., Prélat, A., Box, D., Di Celma, C. N. & Kavanagh, J. P., 2011. Depositional architecture and sequence stratigraphy of the Karoo basin floor to shelf edge succession, Laingsburg depocentre, South Africa. Marine and Petroleum Geology, 28 (3), pp. 658-674.

Flood, R. D., Manley, P. L., Kowsmann, R. O., Appi, C. J. & Pirmez, C., 1991. Seismic facies and late Quaternary growth of Amazon submarine fan. In: Weimer, P. and Link, M. H. (Eds). Seismic facies and sedimentary processes of submarine fans and turbidite systems, New York, NY, United States, Springer-Verlag, p. 415-433.

Folk, R.L., 1980. Petrology of Sedimentary Rocks. Hemphill, Austin, p.182.

Fonnesu, M., Felletti, F., Haughton, P. D., Patacci, M. & McCaffrey, W. D., 2018. Hybrid event bed character and distribution linked to turbidite system sub- environments: The North Apennine Gottero Sandstone (north- west Italy). Sedimentology, 65, p. 151-190

Gamberi, F., Rovere, M., Dykstra, M., Kane, I. A. & Kneller, B. C., 2013. Integrating modern seafloor and outcrop data in the analysis of slope channel architecture and fill. Marine and Petroleum Geology, 41, p. 83-103.

Gardner, M. H. & Borer, J. M., 2000. Submarine channel architecture along a slope to basin profile, Brushy canyon formation, West Texas in Bouma, A. H. and Stone, C. G., eds., Fine-grained turbidite systems, AAPG Memoir 72/SEPM Special Publication 68, p.195–214.

Gardner, M.H., Borer, J.M., Melik, J.J., Mavilla, N., Dechesne, M. & Wagerle, R.D., 2003. Stratigraphic process-response model for submarine channels and related features from studies of Permian Brushy Canyon outcrops, West Texas. Marine and Petroleum Geology, 20, 757–788.

Geehan, G. & Underwood, J., 1993. The use of length distributions in geological modelling. In: Flint, S.S. & Bryant, I.D. (Eds.), The geological modelling of hydrocarbon reservoirs and outcrop analogues, 15, IAS Special Publication, p. 205-212.

Gervais, A., Mulder, T., Savoye, B. & Gonthier, E., 2006(a). Sediment distribution and evolution of sedimentary processes in a small sandy turbidite system (Golo system, Mediterranean Sea): implications for various geometries based on core framework. Geo-Marine Letters, 26, (6), p. 373-395.

Gervais, A., Savoye, B., Mulder, T. & Gonthier, E., 2006(b). Sandy modern turbidite lobes: A new insight from high resolution seismic data. Marine and Petroleum Geology, 23, (4), p. 485-502.

Goldhammer, R. K., Wickens, H. d. V., Bouma, A. H. & Wach, G., 2000. Sequence stratigraphic architecture of the Late Permian Tanqua submarine fan complex, Karoo Basin, South Africa. In: Bouma, A. H. & Stone, C. G. (Eds). Fine-grained turbidite systems. AAPG Memoir 72/SEPM Special Publication, 68, pp. 165-171.

Grecula, M., Flint, S. S., Wickens, H. d. V. & Johnson, S. D., 2003. Upward-thickening patterns and lateral continuity of Permian sand-rich turbidite channel fills, Laingsburg Karoo, South Africa. Sedimentology, 50 (5), pp. 831-853.

Hadler-Jacobsen, F., Johannessen, E. P., Ashton, N., Henriksen, S., Johnson, S. D. & Kristensen, J. B., 2005. Submarine fan morphology and lithology distribution: a predictable function of sediment delivery, gross shelf-to-basin relief, slope gradient and basin topography. In: Dore, A. G. and Vining, B. A. (Eds). Petroleum Geology: North-West Europe and Global Perspectives - Proceedings of the 6th Petroleum Geology Conference, p. 1121-1145.

Hall, R., 2013. Contraction and extension in northern Borneo driven by subduction rollback. Journal of Asian Earth Sciences, 76, p. 399-411.

Hansen, L., Janocko, M., Kane, I. & Kneller, B., 2017(a). Submarine channel evolution, terrace development, and preservation of intra-channel thin-bedded turbidites: Mahin and Avon channels, offshore Nigeria. Marine Geology, 383, p. 146-167.

Hansen, L., Callow, R., Kane, I. & Kneller, B., 2017(b). Differentiating submarine channel-related thin-bedded turbidite facies: Outcrop examples from the Rosario Formation, Mexico. Sedimentary Geology, 358, p. 19-34.

Haughton, P. D. W., Davis, C., McCaffrey, W. D. & Barker, S., 2009. Hybrid sediment gravity flow deposits - Classification, origin and significance. Marine and Petroleum Geology, 26, (10), p. 1900-1918.

Hodgson, D. M., Flint, S. S., Hodgetts, D., Drinkwater, N. J., Johannessen, E. P. & Luthi, S. M., 2006. Stratigraphic evolution of fine-grained submarine fan systems, Tanqua depocenter, Karoo Basin, South Africa. Journal of Sedimentary Research, 76 (1-2), pp. 20-40.

Hofstra, M., Hodgson, D. M., Peakall, J. & Flint, S. S., 2015. Giant scour-fills in ancient channel-lobe transition zones: Formative processes and depositional architecture. Sedimentary Geology, 329, pp. 98-114.

Hofstra, M., 2016. The stratigraphic record of submarine channel-lobe transition zones. PhD Thesis, University of Leeds, UK.

Hubbard, S. M., Covault, J. A., Fildani, A. & Romans, B. W., 2014. Sediment transfer and deposition in slope channels: Deciphering the record of enigmatic deep-sea processes from outcrop. Geological Society of America Bulletin, 126, (5-6), p. 857-871.

Ingersoll, R.V., 2012. Chapter 1 - Tectonics of sedimentary basins, with revised nomenclature. In: Tectonics of Sedimentary Basins: Recent Advances, Busby, C. and Azor, A. (eds.), John Wiley & Sons, Ltd, Chichester, UK.

Jegou, I., Savoye, B., Pirmez, C. & Droz, L., 2008. Channel-mouth lobe complex of the recent Amazon Fan: The missing piece. Marine Geology, 252, (1-2), p. 62-77.

Jobe, Z. R., Howes, N. C. & Auchter, N. C., 2016. Comparing submarine and fluvial channel kinematics: Implications for stratigraphic architecture. Geology, 44, (11), p. 931-934.

Kane, I. A., Kneller, B. C., Dykstra, M., Kassem, A. & McCaffrey, W. D., 2007. Anatomy of a submarine channel-levee: An example from Upper Cretaceous slope sediments, Rosario Formation, Baja California, Mexico. Marine and Petroleum Geology, 24, p. 540-563.

Kane, I. A., Dykstra, M., Kneller, B. C., Tremblay, S. & McCaffrey, W. D., 2009. Architecture of a coarse-grained channel-levee system: the Rosario Formation, Baja California, Mexico. Sedimentology, 56, (7), p. 2207-2234.

Kane, I. A. & Hodgson, D. M., 2011. Sedimentological criteria to differentiate submarine channel levee sub-environments: Exhumed examples from the Rosario Fm. (Upper Cretaceous) of Baja California, Mexico, and the Fort Brown Fm. (Permian), Karoo Basin, S. Africa. Marine and Petroleum Geology, 28, (3), p. 807-823.

Kane, I. A., Ponten, A. S. M., Vangdal, B., Eggenhuisen, J. T., Hodgson, D. M. & Spychala, Y. T., 2017. The stratigraphic record and processes of turbidity current transformation across deep-marine lobes. Sedimentology, 64 (5), pp. 1236-1273.

Khan, Z. A. & Arnott, R. W. C., 2011. Stratal attributes and evolution of asymmetric inner- and outer-bend levee deposits associated with an ancient deep-water channel-levee complex within the Isaac Formation, southern Canada. Marine and Petroleum Geology, 28, (3), p. 824-842.

King, P.R. & Trasher, G.P., 1992. Post-Eocene development of the Taranaki basin, New Zealand: Convergent overprint of a passive margin. In: Watkins, J.S., Zhiqiang, F. & McMillen, K.J. (Eds.) Geology and Geophysics of Continental Margins. AAPG Memoirs, 53, p. 93-118.

King, P. R., Browne, G. H. & Slatt, R. M., 1994. Sequence architecture of exposed Late Miocene basin floor fan and channel-levee complexes (Mount Messenger Formation), Taranaki basin, New Zealand. In: Weimer, P., Bouma, A. H. & Perkins, B. (Eds). GCSSEPM Foundation 15th Annual Research Conference, Submarine Fans and Turbidite Systems: Sequence Stratigraphy, Reservoir Architecture and Production Characteristics, Gulf of Mexico and International., Houston, Tex., United States, GCSSEPM Foundation, p. 177-192.

King, E. L., Sejrup, H. P., Haflidason, H., Elverhoi, A. & Aarseth, I., 1996. Quaternary seismic startigraphy of the North Sea Fan: glacially-fed gravity flow aprons, hemipelagic sediments, and large submarine slides. Marine Geology, 130, p. 293-315.

King, P. R., Browne, G. H., Arnot, M. J., Slatt, R. M., Helle, K. & Stromsoyen, I., 2007(a). An Overview of the Miocene Mount Messenger-Urenui Formations, New Zealand: A 2-D, Oblique-dip Outcrop Transect: Through an Entire Third-order, Progradational, Deep-water Clastic Succession. In: Nilsen, T. H., Shew, R. D., Steffens, G. S. and Studlick, J. R. J. (Eds). Atlas of Deep-Water Outcrops. AAPG Studies in Geology, 56, p. 238-240.

King, P. R., Brown, G. H., Arnot, M. J. & Stromsoyen, I., 2007(b). Slope feeder channels, Urenui Formation, Wai-iti and Mimi Beaches, New Zealand. In: Nilsen, T. H., Shew, R. D., Steffens, G. S. and Studlick, J. R. J. (Eds). Atlas of Deep-Water Outcrops. AAPG Studies in Geology, 56, p. 262-264.

King, P. R., Browne, G. H., Arnot, M. J. & Crundwell, M. P., 2007(c). A 2-D, Oblique-dip Outcrop Transect through a Third-order, Progradational, Deep-water Clastic Succession, Urenui-Mount Messenger Formations, New Zealand. In: Nilsen, T. H., Shew, R. D., Steffens, G. S. & Studlick, J. R. J. (Eds). Atlas of Deep-Water Outcrops, CD-ROM. AAPG Studies in Geology, 56, p. 1-42.

King, R. C., Hodgson, D. M., Flint, S. S., Potts, G. J. & Van Lente, B., 2009. Development of subaqueous fold belts as a control on the timing and distribution of deepwater sedimentation: An example from the Southwest Karoo Basin, South Africa. In: Kneller, B. C., Martinsen, O. J. & McCaffrey, W. D. (Eds). External Controls on Deep-Water Depositional Systems. Society for Sedimentary Geology Special Publication, 92, pp. 261-278.

King, P. R., Ilg, B. R., Arnot, M., Browne, G. H., Strachan, L. J., Crundwell, M. P. & Helle, K., 2011. Outcrop and seismic examples of mass-transport deposits from a late Miocene deep-water succession, Taranaki Basin, New Zealand. In: Shipp, R. C., Weimer, P. & Posamentier, H. W. (Eds). Mass-Transport Deposits in Deepwater Settings. Society for Sedimentary Geology Special Publication, United States (USA), Society for Sedimentary Geology (SEPM), Tulsa, OK, United States (USA), p. 311-350.

Konsoer, K., Zinger, J. and Parker, G., 2013. Bankfull hydraulic geometry of submarine channels created by turbidity currents: Relations between bankfull channel characteristics and formative flow discharge. Journal of Geophysical Research: Earth Surface, 118, p.216–228.

Li, P., Kneller, B. C., Hansen, L. & Kane, I. A., 2016. The classical turbidite outcrop at San Clemente, California revisited: An example of sandy submarine channels with asymmetric facies architecture. Sedimentary Geology, 346, p. 1-16.

Li, P., Kneller, B., Thompson, P., Bozetti, G. and dos Santos, T., 2018. Architectural and facies organisation of slope channel fills: Upper Cretaceous Rosario Formation, Baja California, Mexico. Marine and Petroleum Geology, 92, p.632-649.

Macauley, R. V. & Hubbard, S. M., 2013. Slope channel sedimentary processes and stratigraphic stacking, Cretaceous Tres Pasos Formation slope system, Chilean Patagonia. Marine and Petroleum Geology, 41, p. 146-162.

MacDonald, D. I. M., Butterworth, P. J. & Crame, J. A., 1995. Deep marine slide and channel deposits from the Jurassic-Cretaceous Fossil Bluff Group. Alexander Island, Antarctica. In: Pickering, K. T., Hiscott, R. N., Kenyon, N. H., Lucchi, F. R. & Smith, R. D. A. (Eds). Atlas of Deep Water Environments; Architectural Style in Turbidite systems. Chapman and Hall, p. 50-55.

Macdonald, H. A., Peakall, J., Wignall, P. B. & Best, J. L., 2011. Sedimentation in deep-sea lobe-elements: implications for the origin of thickening-upward sequences. Journal of the Geological Society of London, 168, (2), p. 319-331.

Marsset, T., Droz, L., Dennielou, B. & Pichon, E., 2009. Cycles in the architecture of the Quaternary Zaire turbidite system: A possible link with climate. In: Kneller, B. C., Martinsen, O. J. & McCaffrey, W. D. (Eds). External Controls on Deep-Water Depositional Systems. Society for Sedimentary Geology Special Publication, 92, p. 89-106.

Masalimova, L. U., Lowe, D. R., Sharman, G. R., King, P. R. & Arnot, M. J., 2016. Outcrop characterization of a submarine channel-lobe complex: The Lower Mount Messenger Formation, Taranaki Basin, New Zealand. Marine and Petroleum Geology, 71, p. 360-390.

May, J. A. & Warme, J. E., 2007. A rare exposure of an ancient submarine canyon, Black's Beach, California, USA. In: Nilsen, T. H., Shew, R. D., Steffens, G. S. and Studlick, J. R. J. (Eds). Atlas of Deep-Water Outcrops. AAPG Studies in Geology, 56, p. 378-382.

Mayall, M., Jones, E. & Casey, M., 2006. Turbidite channel reservoirs - Key elements in facies prediction and effective development. Marine and Petroleum Geology, 23, (8), p. 821-841.

McArthur, A. D., Kneller, B. C., Souza, P. A. & Kuchle, J., 2016. Characterization of deep-marine channel-levee complex architecture with palynofacies: An outcrop example from the Rosario Formation, Baja California, Mexico. Marine and Petroleum Geology, 73, p. 157-173.

McCaffrey, W. D., Gupta, S. & Brunt, R., 2002. Repeated cycles of submarine channel incision, infill and transition to sheet sandstone development in the Alpine foreland basin, SE France. Sedimentology, 49, (3), p. 623-635.

McHargue, T., Pyrcz, M. J., Sullivan, M. D., Clark, J. D., Fildani, A., Romans, B. W., Covault, J. A., Levy, M., Posamentier, H. W. & Drinkwater, N. J., 2011(a). Architecture of turbidite channel systems on the continental slope: Patterns and predictions. Marine and Petroleum Geology, 28, (3), p. 728-743.

McHargue, T., Pyrcz, M. J., Sullivan, M. D., Clark, J. D., Fildani, A., Levy, M., Drinkwater, N. J., Posamentier, H. W., Romans, B. W. & Covault, J. A., 2011(b). Event-based modeling of turbidite channel fill, channel stacking pattern, and net sand volume. In: Outcrops Revitalized: Tools, Techniques and Applications. SEPM Concepts in Sedimentology and Paleontology, SEPM (Society for Sedimentary Geology), 10, p. 163-173.

Miall, A.D., 1985. Architectural-element analysis: a new method of facies analysis applied to fluvial deposits. Earth-Sci. Rev. 22, 261–308.

Miller, S. & MacDonald, D.I.M., 2004. Metamorphic and thermal history of a fore-arc basin: the Fossil Bluff group, Alexander Island, Antarctic. Journal of Petrology, 45, (7), p.1453-1465.

Moody, J.D., 2010. Effect of growth structures on slope channel architecture and facies with respect to reservoir characterisation, Eocene Morillo Turbidite System (South-Central Pyrenees, Spain). Msc. Thesis, Colorado School of Mines.

Moody, J. D., Pyles, D. R., Clark, J. D. & Bouroullec, R., 2012. Quantitative outcrop characterization of an analog to weakly confined submarine channel systems: Morillo 1 member, Ainsa Basin, Spain. AAPG Bulletin, 96, (10), p. 1813-1841.

Morris, W. R. & Busby Spera, C. J., 1988. Sedimentologic evolution of a submarine canyon in a forearc basin, Upper Cretaceous Rosario Formation, San Carlos, Mexico. AAPG Bulletin, 72, p. 717-737.

Morris, W. & Busby Spera, C. J., 1990. A submarine-fan valley-levee complex in the Upper Cretaceous Rosario Formation; implication for turbidite facies models. Geological Society of America Bulletin, 102, (7), p. 900-914.

Morris, E., 2014. Stratigraphic record of sedimentary processes in submarine channel-levee systems. PhD Thesis, University of Leeds, UK.

Morris, E. A., Hodgson, D. M., Flint, S., Brunt, R. L., Luthi, S. M. & Kolenberg, Y., 2016. Integrating outcrop and subsurface data to assess the temporal evolution of a submarine channel-levee system. AAPG Bulletin, 100 (11), pp. 1663-1691.

Moscardelli, L. & Wood, L., 2015. Morphometry of mass-transport deposits as a predictive tool. Geological Society of America Bulletin, 128, (1-2), p. 47-80.
Mulder, T. & Alexander, J., 2001. The physical character of subaqueous sedimentary density flows and their deposits. Sedimentology, 48, (2), p. 269-299.

Mulder, T. & Alexander, J., 2001. The physical character of subaqueous sedimentary density flows and their deposits. Sedimentology, 48, (2), p. 269-299.

Mutti, E. & Normark, W.R., 1987. Comparing Examples of Modern and Ancient Turbidite Systems: Problems and Concepts. In Leggett, J.K. & Zuffa, G.G. (eds.), Marine clastic sedimentology: concepts and case studies: London, Graham and Troutman, p. 1–38.

Nakajima, T. and Kneller, B. C., 2013. Quantitative analysis of the geometry of submarine external levees. Sedimentology, 60, p.877-910.

Navarro, L., Khan, Z. & Arnott, R. W. C., 2007(a). Depositional Architecture and Evolution of a Deep-marine Channel-levee Complex: Isaac Formation (Windermere Supergroup), Southern Canadian Cordillera. In: Nilsen, T. H., Shew, R. D., Steffens, G. S. & Studlick, J. R. J. (Eds). Atlas of Deep-Water Outcrops, CD-ROM. AAPG Studies in Geology, 56, p. 1-22.

Navarro, L., Khan, Z. A. & Arnott, R. W. C., 2007(b). Architecture of a deep-water channel-levee complex: Channel 3, Castle Creek South, Isaac Formation, Windermere Supergroup, British Columbia, Canada. In: Nilsen, T. H., Shew, R. D., Steffens, G. S. and Studlick, J. R. J. (Eds). Atlas of Deep-Water Outcrops. AAPG Studies in Geology, 56, p. 93-96.

Normark, W. R. & Piper, D. J. W., 1991. Initiation processes and flow evolution of turbidity currents; implications for the depositional record. In: Osborne, R. H. (Eds). From shoreline to abyss; contributions in marine geology in honor of Francis Parker Shepard. Special Publication - Society of Economic Paleontologists and Mineralogists, Tulsa, OK, United States, SEPM (Society for Sedimentary Geology), 46, p. 207-230.

Normark, W. R., Piper, D. J. W. & Hiscott, R. N., 1998. Sea level controls on the textural characteristics and depositional architecture of the Hueneme and associated submarine fan systems, Santa Monica Basin, California. Sedimentology, 45, (1), p. 53-70.

Normark, W. R., Piper, D. J. W., Romans, B. W., Covault, J. A., Dartnell, P. & Sliter, R. W., 2009. Submarine canyon and fan systems of the California Continental Borderland. In: Lee, H. J. and Normark, W. R. (Eds). Earth Science in the Urban Ocean: The Southern California Continental Borderland. Geological Society of America Special Papers, Boulder, 454, p. 141-168.

O'Byrne, C. J., Barton, M. D., Prather, B., Pirmez, C., Sylvester, Z., Commins, D. & Coffa, A., 2007(a). Deep-water channel-complex architectures, Popo Fault Block, Brushy Canyon Formation, Texas, USA - Part 1: stratal framework. In: Nilsen, T. H., Shew, R. D., Steffens, G. S. and Studlick, J. R. J. (Eds). Atlas of Deep-Water Outcrops. AAPG Studies in Geology, 56, p. 457-462.

O'Byrne, C. J., Barton, M. D., Steffens, G. S., Pirmez, C. & Buergisser, H., 2007 (b). Architecture of a laterally migrating channel complex: Channel 4, Isaac Formation, WIndermere Supergroup, Castle Creek North, British Columbia. In: Nilsen, T. H., Shew, R. D., Steffens, G. S. and Studlick, J. R. J. (Eds). Atlas of Deep-Water Outcrops. AAPG Studies in Geology, 56, p. 115-118.

Olabode, S. O. & Adekoya, J. A., 2008. Seismic stratigraphy and development of Avon canyon in Benin (Dahomey) basin, southwestern Nigeria. Journal of African Earth Sciences, 50, (5), p. 286-304.

Pichevin, L., Mulder, T., Savoye, B., Gervais, A., Cremer, M. & Piper, D. J. W., 2003. The Golo submarine turbidite system (east Corsica margin): morphology and processes of terrace formation from high-resolution seismic reflection profiles. Geo-Marine Letters, 23, (2), 117-124.

Pickering, K. T., Hiscott, R. N. & Hein, F. J., 1989. Deep Marine Environments: Clastic Sedimentation and Tectonics. London, Unwin Hyman.

Pickering, K.T., Clark, J.D., Smith, R.D.A., Hiscott, R.N., Ricci Lucchi, F. & Kenyon, N.H., 1995. Architectural element analysis of turbidite systems, and selected topical problems for sand-prone deep-water systems. In: Pickering, K.T., Hiscott, R.N., Kenyon, N.H., Ricci Lucchi, F., Smith, R.D.A. (Eds.), Atlas of Deep Water Environments: Architectural Style in Turbidite Systems. Chapman & Hall, London, pp. 1–10.

Pickering, K. T. & Cantalejo, B., 2015. Deep-marine environments of the Middle Eocene Upper Hecho Group, Spanish Pyrenees: Introduction. Earth-Science Reviews, 144, p. 1-9.

Pickering, K. T., Corregidor, J. & Clark, J. D., 2015. Architecture and stacking patterns of lower-slope and proximal basin-floor channelised submarine fans, Middle Eocene Ainsa System, Spanish Pyrenees: An integrated outcrop-subsurface study. Earth-Science Reviews, 144, p. 47-81.

Picot, M., Droz, L., Marsset, T., Dennielou, B. & Bez, M., 2016. Controls on turbidite sedimentation: Insights from a quantitative approach of submarine channel and lobe architecture (Late Quaternary Congo Fan). Marine and Petroleum Geology, 72, p. 423-446.

Piper, D. J. W., Hiscott, R. N. & Normark, W. R., 1999. Outcrop-scale acoustic facies analysis and latest Quaternary development of Hueneme and Dume submarine fans, offshore California. Sedimentology, 46, (1), p. 47-78.

Piper, D. J. W. & Normark, W. R., 2001. Sandy fans; from Amazon to Hueneme and beyond. AAPG Bulletin, 85, (8), p. 1407-1438.

Posamentier, H. W, 2003. Depositional elements associated with a basin floor channel-levee system: case study from the Gulf of Mexico. Marine and Petroleum Geology, 20, (6-8), p. 677-690.

Posamentier, H. W. & Kolla, V., 2003. Seismic geomorphology and stratigraphy of depositional elements in deep-water settings. Journal of Sedimentary Research, 73, (3), p. 367-388.

Posamentier, H.W. & Walker, R.G., 2006. Deep-water turbidites and submarine fans. In: Posamentier, H.W. & Walker, R.G. (eds), Facies Models Revisited. SEPM Special Publications, 84, p. 399 – 520.

Prather, B. E., 2003. Controls on reservoir distribution, architecture and stratigraphic trapping in slope settings. Marine and Petroleum Geology, 20, (6-8), p. 529-545.

Prather, B. E., Pirmez, C. & Winker, C. D., 2012. Stratigraphy of Linked Intraslope Basins: Brazos-Trinity System Western Gulf of Mexico. In: Prather, B. E., Deptuck, M. E., Mohrig, D., Van Hoorn, B. & Wynn, R. B. (Eds). Application of the Principles of Seismic Geomorphology to Continental-Slope and Base-of-Slope Systems: Case Studies from Seafloor and Near-Seafloor Analogues. SEPM Special Publication, 99, p. 83-109.

Prélat, A., Hodgson, D. M. & Flint, S. S., 2009. Evolution, architecture and hierarchy of distributary deep-water deposits: a high-resolution outcrop investigation from the Permian Karoo Basin, South Africa. Sedimentology, 56 (7), pp. 2132-2154.

Prélat, A., Covault, J. A., Hodgson, D. M., Fildani, A. & Flint, S. S., 2010. Intrinsic controls on the range of volumes, morphologies, and dimensions of submarine lobes. Sedimentary Geology, 232, (1-2), p. 66-76.

Prélat, A. & Hodgson, D. M., 2013. The full range of turbidite bed thickness patterns in submarine lobes: controls and implications. Journal of the Geological Society of London, 170 (1), pp. 209-214.

Pringle, J. K., Brunt, R. L., Hodgson, D. M. & Flint, S. S., 2010. Capturing stratigraphic and sedimentological complexity from submarine channel complex outcrops to digital 3D models, Karoo Basin, South Africa. Petroleum Geoscience, 16 (4), pp. 307-330.

Pyles, D. R., 2007. Architectural Elements in a Ponded Submarine Fan, Carboniferous Ross Sandstone, Western Ireland. In: Nilsen, T. H., Shew, R. D., Steffens, G. S. and Studlick, J. R. J. (Eds). Atlas of Deep-Water Outcrops, CD-ROM. AAPG Studies in Geology, 56, p. 1-19.

Pyles, D. R., Jennette, D. C., Tomasso, M., Beaubouef, R. T. & Rossen, C., 2010. Concepts learned from a 3D outcrop of a sinuous slope channel complex; Beacon Channel Complex, Brushy Canyon Formation, West Texas, U.S.A. Journal of Sedimentary Research, 80, (1-2), p. 67-96.

Qin, Y. P., Alves, T. M., Constantine, J. & Gamboa, D., 2016. Quantitative seismic geomorphology of a submarine channel system in SE Brazil (Espirito Santo Basin): Scale comparison with other submarine channel systems. Marine and Petroleum Geology, 78, p. 455-473.

Reading, H.G. & Richards, M., 1994. Turbidite systems in deep-water basin margins classified by grain size and feeder system. AAPG Bulletin, 78, (5), p. 792-822.

Richards, M. & Bowman, M., 1998. Submarine fans and related systems II: variability in reservoir architecture and wireline log character. Marine and Petroleum Geology, 15, (8), p. 821-839.

Riley, T.R., Flowerdew, M.J. and Whitehouse, M.J., 2012. Chrono- and lithostratigraphy of a Mesozoic-Tertiary fore-to intra-arc basin: Adelaide Island, Antarctic Peninsula. Geological Magazine, 149, (5), p. 768-782.

Romans, B. W., Fildani, A., Hubbard, S. M., Covault, J. A., Fosdick, J. C. & Graham, S. A., 2011. Evolution of deep-water stratigraphic architecture, Magallanes Basin, Chile. Marine and Petroleum Geology, 28, (3), p. 612-628.

Ross, G. M. & Arnott, R. W. C., 2007. Regional Geology of the Windermere Supergroup, Southern Canadian Cordillera and Stratigraphic Setting of the Castle Creek Study Area, Canada. In: Nilsen, T. H., Shew, R. D., Steffens, G. S. & Studlick, J. R. J. (Eds). Atlas of Deep-Water Outcrops, CD-ROM. AAPG Studies in Geology, 56, p. 1-16.

Rotzien, J. R., Lowe, D. R., King, P. R. & Browne, G. H., 2014. Stratigraphic architecture and evolution of a deep-water slope channel-levee and overbank apron: The Upper Miocene Upper Mount Messenger Formation, Taranaki Basin. Marine and Petroleum Geology, 52, p. 22-41.

Saller, A. H., Noah, J. T., Ruzuar, A. P. & Schneider, R., 2004. Linked lowstand delta to basin floor fan deposition, offshore Indonesia: An analog for deep-water reservoir systems. AAPG Bulletin, 88, (1), p. 21-46.

Saller, A., Werner, K., Sugiaman, F., Cebastiant, A., May, R., Glenn, D. & Barker, C., 2008. Characteristics of Pleistocene deep-water fan lobes and their application to an upper Miocene reservoir model, offshore East Kalimantan, Indonesia. AAPG Bulletin, 92, (7), p. 919-949.

Schwarz, E. & Arnott, R. W. C., 2007. Anatomy and evolution of a slope channel-complex set (Neoproterozoic Isaac Formation, Windermere supergroup, southern Canadian cordillera): Implications for reservoir characterization. Journal of Sedimentary Research, 77, (1-2), p. 89-109.

Scotchman, J. I., Bown, P., Pickering, K. T., BouDagher-Fadel, M., Bayliss, N. J. & Robinson, S. A., 2015. A new age model for the middle Eocene deep-marine Ainsa Basin, Spanish Pyrenees. Earth-Science Reviews, 144, p. 10-22.

Shanmugam, G. & Moiola, R. J., 1988. Submarine fans: characteristics, models, classification, and reservoir potential. Earth-Science Reviews, 24, (6), p. 383-428.

Sixsmith, P. J., Flint, S. S., Wickens, H. d. V. & Johnson, S. D., 2004. Anatomy and stratigraphic development of a basin floor turbidite system in the Laingsburg Formation, Main Karoo Basin, South Africa. Journal of Sedimentary Research, 74 (2), pp. 239-254.

Skene, K. I., Piper, D. J. W. and Hill, P. S., 2002. Quantitative analysis of variations in depositional sequence thickness from submarine channel levees. Sedimentology, 49, p.1141-1430.

Slatt, R. M., 2000. Why Outcrop Characterization of Turbidite Systems. In: Bouma, A. H. & Stone, C. G. (Eds). Fine-grained turbidite systems. AAPG Memoir 72/SEPM Special Publication, 68, p.181-186.

Sømme, T. O., Piper, D. J. W., Deptuck, M. E. & Helland-Hansen, W., 2011. Linking onshore-offshore sediment dispersal in the Golo source-to-sink system (Corsica, France) during the Late Quaternary. Journal of Sedimentary Research, 81, (1-2), p. 118-137.

Sprague, A. R. G., Garfield, T. R., Goulding, F. J., Beaubouef, R. T., Sullivan, M. D., Rossen, C., Campion, K. M., Sickafoose, D. K., Abreu, V., Schellpeper, M. E., Jensen, G. N., Jennette, D. C., Pirmez, C., Dixon, B. T., Ying, D., Ardill, J., Mohrig, D. C., Porter, M. L., Farrell, M. E. & Mellere, D., 2005. Integrated Slope Channel Depositional Models: The Key to Successful Prediction of Reservoir Presence and Quality in Offshore West Africa. In: CIPM - E-Exitep 2005, Feb 20-23, 2005, Veracruz, México, p. 1-13.

Spychala, Y. T., Hodgson, D. M., Stevenson, C. J. & Flint, S. S., 2017(a). Aggradational lobe fringes: The influence of subtle intrabasinal seabed topography on sediment gravity flow processes and lobe stacking patterns. Sedimentology, 64 (2), pp. 582-608.

Spychala, Y. T., Hodgson, D. M. & Lee, D. R., 2017(b). Autogenic controls on hybrid bed distribution in submarine lobe complexes. Marine and Petroleum Geology, 88, pp. 1078-1093.

Stöckli, R., Vermote, E., Saleous, N., Simmon, R. and Herring, D., 2005.
The Blue Marble Next Generation - A true color earth
dataset including seasonal dynamics from MODIS. NASA Earth Observatory. Available at: https://visibleearth.nasa.gov/view.php?id=73826. [Accessed 10 May 2018].

Stow, D.A.V. & Mayall, M., 2000. Deep-water sedimentary systems: New models for the 21st century. Marine and Petroleum Geology, 17, p. 125-135

Straub, K. M. & Pyles, D. R., 2012. Quantifying the Hierarchical Organization of Compensation in Submarine Fans Using Surface Statistics. Journal of Sedimentary Research, 82, p. 889-898.

Stright, L., Stewart, J., Campion, K. & Graham, S., 2014. Geologic and seismic modeling of a coarse-grained deep-water channel reservoir analog (Black's Beach, La Jolla, California). AAPG Bulletin, 98, (4), p. 695-728.

Sugiaman, F., Cebastiant, A., Werner, K., Saller, A., Glenn, D. & May, R., 2007. Reservoir characterisation and modelling of an upper Miocene deepwater fan reservoir, Gendalo field, Kutai basin, offshore east Kalimantan. Indonesian Petroleum Association, 31st Annual Convention & Exhibition, May 2007.

Terlaky, V., Rocheleau, J. & Arnott, R.W.C., 2016. Stratal composition and stratigraphic organisation of stratal elements in an ancient deep-marine basin-floor succession, Neoproterozoic Windermere Supergroup, British Columbia, Canada. Sedimentology 63 (1), 136–175.

Tucker, M.E., 2011. Sedimentary rocks in the field: a practical guide. 4th Ed. West Sussex, Chichester: Wiley-Blackwell.

Vinnels, J. S., Butler, R. W. H., McCaffrey, W. D. & Lickorish, W. H., 2010. Sediment Distribution and Architecture around a Bathymetrically Complex Basin: an Example from the Eastern Champsaur Basin, Se France. Journal of Sedimentary Research, 80, (3-4), p. 216-235.

Waibel, A.F., 1990. Sedimentology, petrographic variability, and very-low-grade metamorphism of the Champsaur Sandstone (Paleogene, Hautes-Alpes, France). Evolution of Volcaniclastic Foreland Turbidites in the External Western Alps. Doctoral thesis, University of Geneva.

Wentworth, C.K., 1922. A scale of grade and class terms for clastic sediments. The journal of Geology, 30, (5), p. 377-392.

Weimer, P. & Slatt, R. M., 2007a. Overview of Deepwater Reservoir Elements. In: Weimer, P. and Slatt, R. M. (Eds). Introduction to the Petroleum Geology of Deepwater Settings. AAPG Studies in Geology, 57, p. 149-170.

Weimer, P. & Slatt, R. M., 2007b. Deepwater Reservoir Elements: Channels and their Sedimentary Fills. In: Weimer, P. and Slatt, R. M. (Eds). Introduction to the Petroleum Geology of Deepwater Settings. AAPG Studies in Geology, 57, p. 171-276.

Wynn, R. B., Cronin, B. T. & Peakall, J., 2007. Sinuous deep-water channels: Genesis, geometry and architecture. Marine and Petroleum Geology, 24, p. 341-387.

Yang, S.-Y. & Kim, J. W., 2014. Pliocene basin-floor fan sedimentation in the Bay of Bengal (offshore northwest Myanmar). Marine and Petroleum Geology, 49, p. 45-58.

Zhang, L. F., Pan, M. & Wang, H. L., 2017. Deepwater Turbidite Lobe Deposits: A Review of the Research Frontiers. Acta Geologica Sinica-English Edition, 91, (1), p. 283-300.